Università degli Studi di Padova

Sede Amministrativa: Università degli Studi di Padova

Dipartimento di Medicina Molecolare

SCUOLA DI DOTTORATO DI RICERCA IN: BIOMEDICINA
INDIRIZZO: MEDICINA MOLECOLARE
CICLO: XXVIII

YAP/TAZ ACTIVITY AND MECHANISMS OF CELL PLASTICITY

Direttore della Scuola: Ch.mo Prof. Stefano Piccolo
Coordinatore d'indirizzo: Ch.mo Prof. Griorgio Palu'
Supervisore: Ch.mo Prof. Stefano Piccolo

Dottorando: Dr. Lei Chang

INDEX

EXTENDED ABSTRACT

In the last few years, YAP/TAZ emerged as powerful regulators of growth and tumor malignancy. YAP/TAZ are mainly regulated by two inputs: the Hippo pathway and biomechanical pathway. The latter involves structural and physical signals that cells receive from their being attached to the substrate and/or to other cells and that chance the tension and organization of the cytoskeleton and cell shape. In previous works from our laboratory, we indeed found that specific F-actin structures, such as bundled F-actin cables and stress fibers, are required to sustain YAP/TAZ activity. But the cascade intervening between F-actin and YAP/TAZ remains a mystery.

In an independent research line, we also advanced on the biological effects of YAP/TAZ and found that overexpression of YAP in terminally differentiated cells, such as primary neurons, can trigger their dedifferentiation and acquisition of neural stem cells traits. YAP/TAZ can thus overcome the epigenetic barriers associated to terminal differentiation, but the underlying mechanisms are unknown.

The work here described represents both an advancement and a merge of these two research lines. To start, we identified by Mass spectrometry (MS) YAP binding proteins whose interaction is regulated by F-actin. Next, we functionally validated the candidate regulators emerging from this proteomic approach by carrying out siRNA knockdown of the candidates and monitoring the consequences on YAP target gene expression by RT-PCR. Among these functionally validated YAP-binding proteins, our attention was captured by members of the SWI/SNF chromatin-remodeling complex, which includes important tumor suppressors. We confirmed the biochemical interaction between F-actin, SWI/SNF complexes and YAP by independent approaches, and found that YAP interacts with ARID1A. Interestingly, in the presence of F-actin, YAP fails to associate to SWI/SNF factors. At the biological level, we found that

ARID1A and BRM are key element of an epigenetic barrier that preserves the neuronal differentiated state.

ABSTRACT

In the last few years, YAP/TAZ emerged as powerful regulators of growth and tumor malignancy. YAP/TAZ are regulated by two inputs: the Hippo pathway and biomechanical pathway. The latter involves structural and physical signals that cells receive from their being attached to the substrate and/or to other cells and that chance the tension and organization of the cytoskeleton and cell shape. In previous works from our laboratory, we indeed found that specific F-actin structures, such as bundled F-actin cables and stress fibers are required to sustain YAP/TAZ activity. But the cascade intervening between F-actin and YAP/TAZ remains a mystery. In an independent research line, we also advanced on the biological effects of YAP/TAZ and found that overexpression of YAP in terminally differentiated cells, such as primary neurons, can trigger their dedifferentiation and acquisition of stem cells traits. The work here described represents both an advancement and a merge of these two research lines.

SOMMARIO (Italiano)

YAP e TAZ sono stati oggetto di grande attenzione alla luce del loro ruolo come regolatori della proliferazione cellulare. YAP e TAZ sono regolati principalmente da due tipi di segnali: la via di Hippo e la meccanotrasduzione. Quest'ultima comprende genericamente tutta una serie di segnali di contesto che fanno parte della fisicita' e struttura del microambiente, in primis l'attacco delle cellule alla matrice extracellulare ed altre cellule. Questi segnali, hanno la loro natura nelle forze fisiche che le cellule percepiscono e a cui rispondono grazie alla contrattilita' ed organizzazione tridimensionale del citoscheletro. L'equilibrio di queste forze genera la forma della cellula. In precedenti studi, il nostro gruppo ha chiarito come speciali strutture di F-actin siano importanti per l'attivita' o inibizione di YAP/TAZ da parte dell'ambiente. Ma i meccanismi della meccanotrasduzione restano enigmatici. In una linea di ricerca indipendente, abbiamo anche prodotto degli avanzamenti sul ruolo biologico di YAP/TAZ ed una scoperta particolarmente intrigante e' stata che esprimendo YAP (o TAZ) in cellule terminalmente differenziate quali i neuroni si osserva che questi dedifferenziano e diventano molto simili a normali cellule staminali neuronali (NSCs). Il lavoro qui descritto rappresenta sia un avanzamento in queste direzioni di ricerca che un loro inaspettato punto di contatto.

INTRODUCTION

YAP/TAZ and the Hippo pathway

YAP (Yes associated protein) and TAZ (transcriptional coactivator with PDZ-binding motif, also known as WWTR1) are transcriptional modulators that are fundamental to regulate tissue growth and organ size. YAP/TAZ transcriptional activities are regulated by several mechanisms. YAP/TAZ are classically considered to be regulated by the Hippo pathway (Zhao et al., 2011a). The core signaling pathway comprises a cascade of phosphorylations: the Sterile 20-like kinases MST1 and MST2, activated by WW45 (also known as SAV1), in turns directly phosphorylate the large tumor suppressor homolog kinases LAST1/2. LAST1/2 then phosphorylate YAP/TAZ at multiple residues and inactivate them. Indeed, some of these LATS-phosphorylated residues (including YAP Ser127 and TAZ Ser89) have been found to promote 14-3-3 protein binding, as such preventing YAP/TAZ from translocation into the nucleus (Zhao et al., 2011); others have been proved as critical for proteosomal recognition and degradation. Conversely, when the Hippo pathway is not active, unphosphorylated YAP/TAZ can bind to the transcription factors TEAD (TEA domain family member) in the nucleus and promote proliferation or stem cells self renewal (Ramos and Camargo, 2012; Zhang et al., 2009) (**Figure 1A**). However, in recent years, several variations on this basic signaling module have been reported, including LATS-independent phosphorylation of YAP/TAZ, MST-independent activation of LATS, phosphorylation-independent modalities of YAP/TAZ controls and others, such as the Wnt pathway (Azzolin et al., 2012; Shao et al., 2012), the TGF-beta pathway (Varelas et al., 2008) and the GPCR pathway (Yu et al., 2012).

In previous work from our laboratory, we discovered a new mechanism of

YAP/TAZ regulation by extracellular matrix (ECM) and physical/mechanical inputs, operating through the F-actin cytoskeleton (Dupont et al., 2011). As such, the definition of YAP/TAZ as mediators of the Hippo pathway has been progressively changed to include clear non-hippo regulations and probably other pathways feeding on YAP/TAZ activity.

YAP/TAZ and mechanical cues.

One of the most fascinating aspects of YAP/TAZ biology is their regulation by structural elements that originate from the tissue. These can be summarized as: i) the cytoskeleton tension and cell-cell junctions that keep cells, tissues and organs in a certain shape; ii) adhesion of a cell to its surrounding extracellular matrix (ECM) (Halder et al., 2012). These structural elements can inform cells about the status of the tissue in which they are embedded, such as organ size and three-dimensional organization. When cells receive the information from these structural elements, cells regulate the activity of YAP/TAZ to promote proliferation or stem cell self renewal. These regulations offer the unprecedented opportunity to explore one of most mystery events in the biology, that is, wiring signal transduction and cell biology at the tissue level.

YAP and TAZ are regulated by ECM stiffness, cytoskeletal tension and cell shape (Dupont et al., 2011; Wada et al., 2011). When cells are seeded on a stiff ECM, YAP/TAZ are nuclearly localized and transcriptionally active, whereas they are inhibited and relocalized in the cytoplasm when cells are seeded on a soft ECM (Dupont et al., 2011). Cell shape can be controlled by seeding cells on microprinted fibronectin “islands” of different sizes (Chen, 1997). In spread cells (cells growing at low density on plastic dishes, seeded on “big” fibronectin islands or stretched by mechanical force), YAP/TAZ are well active. But when cells grow as small, roundish, or unspread (seeded on small “islands”) units, YAP/TAZ are inactivated (Dupont et al., 2011; Wada et al., 2011; Aragona et al., 2013)(**Figure 1B**).

Crucially, YAP/TAZ are the key mediators in the biological effects of ECM stiffness and cell shape. For example, when forced to remain small, endothelial cells die, while they proliferate when they are allowed to spread (Chen et al., 1997). We can rewrite this behaviors by artificially change YAP/TAZ levels: if YAP/TAZ are artificially increased in small cells, cells start to proliferate; in contrast, attenuation of YAP/TAZ in spread cells causes them to die (Dupont et al., 2011). Contact inhibition of growth of epithelial cells in high cell density is paralleled by YAP/TAZ inhibition. Although traditionally cell-cell contact inhibition is associated to the Hippo cascade, new evidence suggests that contact inhibition may also be considered as a consequence of the reduced cell shape, due to the confinement of cell-ECM adhesion area (reviewed in (Halder et al., 2012)).

Interestingly, the regulation of YAP/TAZ by mechanical cues is different from their regulation by the Hippo pathway. Indeed, lowering mechanical cues leads to YAP/TAZ phosphorylation (degradation) and cytoplasmic relocalization in epithelial, mesenchymal post-EMT cells, as well as in cells expressing LATS insensitive YAP, or depleted of LATS (Dupont et al., 2011; Aragona et al., 2013). Mechanical cues and cell shape are associated to the regulation of the Rho family of small GTPase, of ROCK, MLCK and to corresponding changes in the tensile properties and dynamics of the actomyosin cytoskeleton (Mammoto and Ingber, 2009; Parsons et al., 2010; Wozniak and Chen, 2009). In line with this notion, YAP/TAZ activities are dependent on this cytoskeletal pathway (Dupont et al., 2011; Fernández et al., 2011; Sansores-Garcia et al., 2011; Wada et al., 2011; Zhao et al., 2012). Effective disruption of the F-actin cytoskeleton causes inactivation of YAP/TAZ in a way that is independent from LATS (Dupont et al., 2011). Further more, if we deplete F-actin-capping/severing proteins Cofilin, CapZ, and Gelsolin in cells seeded in lower mechanical cues, YAP/TAZ activity is restored (Aragona et al., 2013). This indicates that cytoskeletal inputs are simply fundamental signals of YAP/TAZ activity, and that, probably, other regulations at the level of the Hippo cascade or other inputs may cooperate or

modify but not overrule the information of the mechanical context (Halder et al., 2012).

The biological functions of YAP/TAZ: growth, cell plasticity and endowing stemness properties

YAP/TAZ are endowed with potent biological properties. YAP/TAZ are well known, at least in cell lines, to be able to overcome inhibition of cell proliferation caused by "contact inhibition"(Gumbiner and Kim, 2014). Mechanistically this is mediated by YAP/TAZ acting directly on enhancers of a host of target genes that control S-phase entry and mitosis (Zanconato et al., 2015). In addition, YAP/TAZ control genes involved in escaping apopotosis and promoting survival (Basu et al., 2003; Huang et al., 2005).

The classic and perhaps more visually revealing phenotype of YAP/TAZ is induction of organ overgrowth. Indeed, inactivation of Hippo pathway components causes organs to grow from fetal development to adulthood well beyond their normal size, generating hearts, livers and stomachs that are manyfold bigger than normal/wild-type organs(Piccolo et al., 2013; Zhao et al., 2011b). Intriguingly, this is reversible, as when YAP/TAZ return to normal levels, the big organ shrinks back to its correct size, losing the excess of cells by apoptosis. It thus appears that an organ can communicate to each of the cells that compile their information on what should be the organ's "correct" size and to proliferate or to stop proliferate depending on whether this inner benchmark is either yet to be reached or has been surpassed. The nature of this information is entirely mysterious, but it is unlikely to be provided by short-range chemical signals, such as diffusible growth factors; moreover diffusion of any chemical entity is unlikely to provide fine-grained spatial control over cell behavior, differentiation and death that instead occur during organ growth and remodeling. In contrast, mechanical signals can travel at great speed and distance due to the pre-stressed and essentially isometric tension of the extracellular matrix and cell cytoskeleton in

constant "tug of war" equilibrium between each other through focal adhesion and adhesive junction. Similar to vibrations of a guitar cord, changes in the cell's local mechanics can resonate through the tissue to be perceived by the whole organ and, *viceversa*, mechanical signals born at the tissue geometrical and architectural level can target each individual cell with nanometer accuracy, for example instructing the proliferation of a specific cell living in a specific mechanical niche (e.g. at a given location within a gland) but not its neighbor. This represents a speculative theory at the moment, but it is nevertheless intriguing that increasing tension in the cytoskeleton of mice lacking the actin severing proteins ADF and cofillin has been associated to dramatic tissue overgrowths (Kanellos et al., 2015).

The role of YAP/TAZ in adult tissues has also started to be explored by using conditional knockouts. The general theme emerging is that, just like YAP/TAZ activation is instrumental for organ growth in embryos, they are dispensable for homeostasis of adult tissues. And, nevertheless, they remain essential for tumorigenesis initiated by loss of Hippo signaling (Cai et al., 2010; Lu et al., 2010), chemical carcinogenesis (Zanconato et al., 2015) and common oncogenic lesions (Da et al., 2009; Lau et al., 2014). On one hand, this specific requirement makes YAP/TAZ very appealing targets for therapeutic intervention. On the other, the relevance of YAP/TAZ is not an invention of cancer cells, but it rather represents the co-option of a physiological function, that is the role of YAP/TAZ for tissue repair. YAP/TAZ are indeed relevant for wound healing in all the tissues in which they have been knocked out: in the intestine, lack of YAP/TAZ causes very rapid cell death because of lack of repair of intestinal mucosa in models of colitis or irradiation (Gregorieff et al., 2015); in the liver, gain-YAP/TAZ triggers repair after chemical injury (Nejak-Bowen et al., 2015) and in the heart, reactivation of YAP/TAZ can regenerate the myocardium after infarction (Lin and Pu, 2014; Xin et al., 2011). The dual requirement of YAP/TAZ in cancer and regeneration is in line with the notion that cancer does not necessarily divert normal stem cell programs, as it is often discussed; rather, it

recapitulates aspect of embryonic or of adult tissues under special conditions, such as stressed, damaged, inflamed tissues that are in fact conditions requiring growth and de novo regrowth, tissue remodeling and cell plasticity. Importantly, evidence exists that "professional" somatic stem cells may not be only or even the leading actors of wound repair (Carlén et al., 2009; Ito et al., 2005); by lineage tracing, it has been demonstrated that the healing microenviroment can actually trigger de-differentiation of committed progenitors, if not fully differentiated cells, back to a stem cell status (Yimlamai et al., 2014a; Zhao et al., 2014). In other words, in order to match its needs, the tissue "calls on stem cell duty" cells that would normally only leave the stem cell niche to differentiate and die, reverting the differentiation process. The mechanisms of this de-differentiation are unknown but certainly entail a combination of chemical (ie. Interleukins, TGFb and other cytokines of the wound healing microenvironment)(Coussens and Werb, 2002; Mast and Schultz, 1996) and physical cues (cell spreading over the exposed ECM, loss of contact inhibition, stiff/activated fibroblasts, de novo deposition of specific matrix protein - such as laminin 11 - all in turn feedbacking on cell contractility and viceversa)(Hashimoto et al., 2004; Tsuruta et al., 2011). The involvement of YAP/TAZ in these events is well-established and may explain why YAP/TAZ are so crucial for repair and cancer: not only they are inhibited by and relevant for contact inhibition and cell mechanical cues, but they may be also fundamental for dedifferentiation and de-novo generation of somatic stem cells from more differentiated cells. The latter is one of the themes of this thesis, for which I collaborated with and build on the work of my colleagues Tito Panciera, Luca Azzolin, Atsushi Fujimura and others, who found that inducing YAP/TAZ expression in differentiated cells of various histotypes induces them to regress to the corresponding lineage-specific somatic stem cell status. YAP/TAZ expression, as shown here, can turn neurons (or astrocytes) into neural stem cells; or turn luminal differentiated cells of the mammary gland into Mammary stem cells, and pancreatic exocrine cells into pancreatic progenitors (**Figure 1C**).

The ability of YAP/TAZ to overcome the barriers of differentiation may occur in vivo, as in livers of transgenic mice the overexpression of YAP transdifferentiated hepatocytes in bile-duct-like cells (Fitamant et al., 2015; Yimlamai et al., 2014b). The role of YAP/TAZ in dedifferentiation also resonates with an even earlier requirement of TAZ in breast cancer. Michelangelo Cordenonsi and colleagues had shown that TAZ expression correlated to cancer stemness genetic signatures; YAP/TAZ are not ubiquitously expressed in tumor cells but are specifically enriched in cancer initiating stem cells (Cordenonsi et al., 2011). Strikingly, expression of TAZ does not simply expand the cancer stem cell populations; rather it converted non-stem tumor cells into cancer stem cells (Cordenonsi et al., 2011). This concept may be actually rephrased in a slightly different way: TAZ expression cause dedifferentiation of more differentiated and more benign tumor cells into their more aggressive and plastic mother cells, expanding their number not (just) by promoting their proliferation but by enlarging their number by cooptation of other cells into a more progenitor-like cellular state. Obviously, these events do not occur randomly or interest all cells, neither in wound healing nor in cancer tissues. YAP/TAZ activity need to be spatially controlled and even in the most aggressive tumors, YAP/TAZ remains dependent on "ground control", that is to the structural features of the specific environment to which they are attached (Zanconato and Piccolo, 2015). In other words, mechanical signals are also important to instruct which cells express sufficient YAP/TAZ to induce them to be stem cells.

These perspectives brings back the focus to what are the signals that are relevant for YAP/TAZ mechanotransduction. And this is the starting point of this thesis. By Mass Spectrometry, we identified SWI/SNF as regulators of YAP/TAZ activity during differentiation and as candidate sensors of mechanotransduction.

SWI/SNF as epigenetic regulators of chromatin structure

There are two classes of complexes regulating chromatin structure: i)

complexes that covalently modify histone tails; and ii) ATP-dependent complexes that remodel nucleosomes. These two classes cooperate to regulate the structure of chromatin dynamically, and thus control gene expression. On the basis of subunit composition and biochemical activity, the ATP-dependent chromatin remodellers can be further divided into families, including SWI/SNF, ISWI, INO80, SWR1 and NURD/Mi2/CHD complexes. Among these, SWI/SNF complexes are emerging as bona fide tumor suppressors, as they have been found to be specifically inactivated by mutations in several human cancers (Wilson and Roberts, 2011).

SWI/SNF chromatin remodeling complexes constitute a highly related family of evolutionarily conserved multisubunit complexes (**Figure 1D**). SWI/SNF complexes have several functions. They modulate gene expression by interacting with transcription factors, coactivators, and corepressors, and they mobilize nucleosomes at target promoters and enhancers (Hu et al., 2011; Tolstorukov et al., 2013; Yu et al., 2013). They also have been implicated in various types of DNA repair (Dykhuizen et al., 2013; Gong et al., 2006; Hara and Sancar, 2002; Park et al., 2006; Watanabe et al., 2014).

SWI/SNF in Cancer

In the late 1990s, the first clue linking SWI/SNF complexes to cancer was the discovery of mutations of SNF5 in rhabdoid tumors (RTs), a rare but highly aggressive type of cancer (Biegel et al., 1999; Versteege et al., 1998). In genetically engineered mouse models, Snf5 was subsequently validated as potent and bona fide tumor suppressor (Guidi et al., 2001a; Roberts et al., 2002) Although this observation has been first noted over a decade ago, only more recently it has been discovered that many types of cancer have SWI/SNF subunit mutations thanks to cancer genome sequencing studies. At least nine genes enconding for subunits of SWI/SNF complexes have been identified as recurrently mutated in cancers derived from nearly every tissue in the body, and

collectively occurring in 20% of all human cancers (Helming et al., 2014; Wilson and Roberts, 2011). The function of mutated SWI/SNF complexes in cancer and the mechanisms by which mutations in individual subunits promote oncogenesis are now active areas of research.

The role of SWI/SNF in lineage specification.

In the lineage-specific differentiation, SWI/SNF complexes play important roles. Essential roles of the SWI/SNF complexes have been identified during neurogenesis, adipogenesis, myogenesis, osteogenesis and haematopoiesis, and the complexes are involved in the differentiation of many other lineages (de la Serna et al., 2006; Flowers et al., 2009; Young et al., 2005). During differentiation, tissue-specific transcription factors cooperate with SWI/SNF complexes to coordinately balance the suppression of proliferation programs and the activation of lineage-specific genes. Despite these roles, how the complexes achieve specific regulation of gene expression remains misty.

It seems that mammalian SWI/SNF complexes are highly heterogeneous, from the point of view of both composition and differential presence in different tissues. In addition to core subunits, which are expressed in all lineages, the SWI/SNF complexes contain variant subunits that is restricted in specific lineages or tissues. For example, it has been discovered that several neural-specific subunits can distinguish post-mitotic mature neurons from neural progenitors. These variant complexes could control gene expression programs, which are required for the neuron terminal differentiation (Lessard et al., 2007; Wu et al., 2007). Based on the large number of subunits, and the tissue-specific composition of the complexes, it has been estimated that hundreds variants of SWI/SNF complexes might exist (Wu et al., 2009), which bind lineage-specific transcription factors and modulate specific loci. Thus, during the control of these developmental programs, specificity of SWI/SNF complexes is achieved in part through restricted expression and in part through combinatorial assembly of

variant SWI/SNF subunits. The BAF60C (SMARCD3) subunit is specifically expressed in the embryonic heart, where it is essential for the cardiac development (Lickert et al., 2004). Similarly, it has been reported that a switch from the BAF45A (PHF10) and BAF53A (ACTL6A) subunits, that are specific expressed in neural progenitors, to BAF45B (DPF1), BAF45C (DPF3), and ACTL6B (BAF53B) subunits is essential during the transition of neural stem cells into post-mitotic neurons (Lessard et al., 2007; Wu et al., 2007). Such switching can facilitates differential activation of transcriptional pathways by modulating its interaction with specific transcription factors (Kadam, 2000).

Analogously, in ES cells there is a unique combination of core SWI/SNF components and associated factors. Through regulating pluripotency and self-renewal, the SWI/SNF complex contribute to the maintenance of this lineage (Gao et al., 2008; Ho et al., 2009; Kidder et al., 2009; Yan et al., 2008). Mouse embryos lacking the SWI/SNF subunits ARID1A, BRG1, SNF5 or BAF155 die near the peri-implantation stage of development, shortly after ES cells are formed (Guidi et al., 2001b; Klochendler-Yeivin et al., 2000; Roberts et al., 2000). In cultured ES cells, inactivation of BRG1 or ARID1A leads to defects in self-renewal and promotes differentiation (Bultman et al., 2000; Ho et al., 2009). As ES cells are the only known cell type in which BAF155 can replace BAF170, a unique subunit composition may contribute to these roles (Ho et al., 2009). This variant complex together with key pluripotency transcription factors, such as OCT4, NANOG and SOX2, co-localize at target gene promoters to facilitate ES cell-specific stem cell gene expression programs (Ho et al., 2009). Moreover, forced overexpression of the core SWI/SNF subunits BAF155 and/or BRG1 enhances the reprogramming of fibroblasts into induced pluripotent stem (iPS) cells (Singhal et al., 2010), where they have been proposed to facilitate the binding of OCT4 to target genes. In primary embryonic fibroblasts, inactivation of Snf5 also leads to the upregulation of stem cell-associated signatures (Wilson et al., 2010). In *Drosophila* neuroblasts, ARID1a (or BRM) induces a transcriptional

program that initiates temporal patterning, limits self-renewal, and prevents dedifferentiation (Eroglu et al., 2014; Koe et al., 2014). Collectively, these studies establish that the SWI/SNF complex work as an important regulator in stem cell self-renewal and pluripotency, and raise the possibility that the oncogenic stimulus due the SWI/SNF mutations may be partly derived from SWI/SNF involvement in regulating the balance between self-renewal and differentiation.

In primary embryonic fibroblasts, inactivation of SNF5 also leads to the upregulation of stem cell-associated signatures (Wilson et al., 2010). In *Drosophila* neuroblasts, ARID1a (or BRM) induces a transcriptional program that initiates temporal patterning, limits self-renewal, and prevents dedifferentiation (Eroglu et al., 2014; Koe et al., 2014). Collectively, these studies establish that the SWI/SNF complex work as an important regulator in stem cell self-renewal and pluripotency, and raise the possibility that the oncogenic stimulus due the SWI/SNF mutations may be partly derived from SWI/SNF involvement in regulating the balance between self-renewal and differentiation.

RESULTS

YAP/TAZ are classically considered to be under the regulation of the Hippo signaling pathway, which culminates in YAP/TAZ phosphorylation by LATS1/2: this event prevents YAP/TAZ translocation into the nucleus (Zhao et al., 2011). Indeed, LATS-phosphorylated YAP/TAZ are cytoplasmic and inactive, whereas unphosphorylated YAP/TAZ escape their cytoplasmic anchors and enters in the nucleus where they can activate target gene expression. However, in previous work from our laboratory, we have established YAP/TAZ as sensors and mediators of mechanotransduction (Aragona et al., 2013; Dupont et al., 2011) in a Hippo-independent manner. We demonstrated that F-actin is the key unit in this pathway, and we identified the F-actin-capping/severing proteins Cofilin, CapZ, and Gelsolin as essential gatekeepers of F-actin-mediated YAP/TAZ regulation (Aragona et al., 2013). Cofilin, CapZ, and Gelsolin inhibit polymerization of F-actin and as such are upstream regulators of F-actin. Thus, the linkage between F-actin and YAP/TAZ still remains unknown. We initiated this study with the aim of identifying the missing linker in the F-actin-regulated YAP/TAZ activity.

YAP/TAZ location does not always mean YAP/TAZ transcription activity

In sparse culture conditions, YAP/TAZ are usually nuclearly localized and active (Dupont et al., 2011). We started our studies by noticing that sparse MCF10A mammary epithelial cells treated with Latrunculin A (0.5 μM, Lat.A), a drug that prevents F-actin assembly, however tend to relocalize YAP/TAZ out of the nucleus. Strickingly, this was dependent on the nuclear export machinery of YAP/TAZ, as concomitant treatment with Leptomycin B (15 ng/mL LMB, an inhibitor of chromosomal region maintenance/exportin1) rescued YAP/TAZ back to the nucleus (**Figure 2A-C**). As the nuclear localization of YAP/TAZ directly reflects their transcriptional activity, we next monitored their capacity to activate

target gene expression by measuring the mRNA level of the established YAP/TAZ targets CYR61 and ANKRD1(Zanconato et al., 2015). As expected, the expression of these genes is high in sparse cells and inhibited with Lat.A, in line with YAP/TAZ localization. However, in Lat.A-treated cells, LMB could not rescue CYR61 and ANKRD1 levels back to control levels, even though YAP/TAZ are nuclear in these conditions (**Figure 2D and 2E**). In conclusion, we found that, in the absence of intact F-actin, even if we artificially rescued YAP/TAZ nuclear localization, YAP/TAZ are still not transcriptionally active.

Nuclear re-localized YAP/TAZ could not rescue mechanical-mediated loss of YAP/TAZ activity

According to our previous work, YAP/TAZ are localized in the cytoplasm and, as such, transcriptionally inactive (Aragona et al., 2013; Dupont et al., 2011) in cells plated on a soft ECM or at high density, two conditions that are highly reminiscent of Lat.A treatment (see **Figure. 2**). Therefore, we wanted to check the effect of LMB on YAP/TAZ localization and activity in cells cultured at high confluence or on soft substrates (**Figure 3A and 4A**). We confirmed that MCF10A cells plated at high confluence or on a soft substrate (hydrogels of 0.7 KPa, kindly prepared by Stefano Giulitti, in the laboratory of prof. Nicola Elvassore, Department of Industrial Engineering, University of Padova) displayed a cytoplasmic immuno-staining of YAP/TAZ and a low expression of their target genes compared to sparse cells or the same cells plated on stiff substrate, respectively (**Figure 3B and 4B**). As for Lat.A, also in these two set-ups, concomitant treatment with LMB could cause YAP/TAZ nuclear accumulation but could not rescue CYR61 and PTX3 expression back to control levels (**Figure 3D-E and Figure 4D-E**). These data clearly demonstrate that in cells plated at high confluence or on soft substrates, as well as upon Lat.A treatment, YAP/TAZ transcriptional activity are inhibited even when YAP/TAZ are inside the nucleus. This suggests the existence of YAP/TAZ nuclear regulators that are under the

mechanical control.

Biochemical screening for YAP/TAZ interactors

Next we sought to identify nuclear regulator(s) of YAP/TAZ that are controlled by mechanical stimuli. Two hypotheses may explain the regulation of YAP/TAZ described in the previous paragraphs by mechanical cues: i) the existence of a protein "X" activated by intact F-actin and required to sustain YAP/TAZ function; the interaction between YAP and protein X is expected to decrease upon F-actin disassembly (i.e. Lat.A treatment); or ii) the existence of a protein "Y" inhibited by F-actin and usually functioning as a natural inhibitor of YAP/TAZ; the interaction between YAP and protein Y therefore is expected to be stabilized by disruption of the F-actin cytoskeleton (**Figure 5A**).

In order to find out this(these) regulatory(ies) factor(s), we sought to identify the YAP/TAZ nuclear binding proteins that are modulated by cytoskeletal properties with a pull-down assay followed by mass spectroscopy. To do it in an unbiased way, we decided to compare the interactors of YAP in cells plated at low confluence with unrestrained adhesive area to those in cells treated with Lat.A, an inhibitor of F-actin formation that is functionally equivalent to mechanical conditions such as a soft ECM or a small ECM island (dense). First, we optimized a pull-down assay to isolate YAP/TAZ together with their interactors in MCF10A cells, as this cell line displays a strong YAP/TAZ regulation by mechanical cues and, in particular, by F-actin cytoskeleton. We used MCF10A cells stably-expressing Flag-tagged YAP 5SA and, as a (negative) control, MCF10A cells transduced with the corresponding empty vector. Both cell lines were left untreated or treated with Lat.A for 4 hours and then harvested (4 samples in total). Extracts were then subjected to anti-Flag IP and Western blot analysis for known interactors of YAP in order to validate our experimental set-up. Indeed, known YAP interacting proteins, such as TEAD1, AMOTL2 and LATS, were readily recovered from the eluate after Flag-YAP immunoprecipitation. To identify all

YAP interactors and especially those whose binding with YAP is sensitive to Lat.A, after immunoprecipitations the eluates were run in a 4-12% gradient SDS-PAGE and the gel was sent to the EMBL core proteomic facility for MS analysis (**Figure 5B**). The details of the preparation of the samples for the mass-spectrometric analysis will not be discussed here. Briefly, each sample lane was cut into five pieces according to molecular weight, and all the proteins contained in each piece subjected to in-gel tryptic digestion. The resulting peptides were purified and subjected to identification based on their mass according to EMBL parameters. We therefore obtained a list of proteins for each sample. From this list, we excluded the proteins aspecifically interacting with the anti-Flag beads used for the immunoprecipitation, that are: i) proteins that were equally represented in the immunoprecipitation from untreated control MCF10A cells and untreated Flag-YAP 5SA-expressing MCF10A cells; ii) proteins that were equally represented in the immunoprecipitation from Lat.A-treated control MCF10A cells and Lat.A-treated Flag-YAP 5SA-expressing MCF10A cells.

As shown in **Table 3**, we could isolate some YAP-interacting proteins so far identified by similar approaches in the literature, like LATS, AMOTL2 and TEAD, that can be considered as positive controls/quality checks of our experiment (**Figure 5C**). Interestingly, we could also detect an interaction between YAP and Merlin/NF2 in extracts from MCF10A cells, likely representing an indirect interaction probably mediated by the LATS kinases (Yin et al., 2013a). Surprisingly, however, we failed to identify in our experiments interaction with MST kinases and Salvador, despite the presence of proteins that have been proposed to act more upstream than MST in the Hippo cascade, such as NF2 which is in line with the discovery with Yin et al. (Yin et al., 2013b). As recently found in Couzens et al., 2013, we also found AMOTL1 and AMOTL2 in our MS approach.

In order to be specific for the interaction, moreover, we set a cut-off to discriminate if a protein can be considered a real interactor of YAP: to do that, we

noticed that known interactors of YAP, such as the TEAD factors, display 4 or more specific peptides in the MS output. We therefore applied this criterion to all the MS results and found some other candidates for YAP interaction, as shown in Table 4. Among all, we looked at the candidates which are more likely sensitive to a regulation by mechanical cues, that are the candidates that display a number of detectable peptides changing between with and without Lat.A. Among these candidates the proteins of the SWI/SNF complex showed good value as YAP regulators. This is because: i) there are several proteins of SWI/SNF complex repeatedly represented in the candidate list (**Table 4**); ii) the ratio of detectable peptides between Flag-YAP-5SA pull down in Lat.A-treated vs Lat.A-untreated cells is high for each individual protein of the SWI/SNF complex; iii) nearly for all the detectable SWI/SNF complex components the binding to YAP in the Lat.A treated samples increases with compared to the untreated sample, suggesting that SWI/SNF might work as an inhibitor; iv) it has been reported that SWI/SNF complex can bind Actin-like proteins (Nishimoto et al., 2012; Rando et al., 2002; Szerlong et al., 2008; Zhao et al., 1998), which suggests its potential in responding to mechanical cues; v) the SWI/SNF complex usually works as regulator in nucleus (Kadoch and Crabtree, 2015; Wilson and Roberts, 2011; Zraly et al., 2006).

Screening of MS results

Next, we decided to validate the results from MS on the SWI/SNF interaction with YAP by loss of function assays. As this is a protein complex, we focused on the core component identified by MS. For this, we used independent siRNAs to treat MCF10A cells in order to knockdown ARID1A, SNF5, BRG1 and BRM endogenous proteins, and to check by qRT-PCR how these knock-downs affect direct YAP/TAZ-regulated genes. As shown in the **Figure 6A-C,** siRNAs against ARID1A and SNF5 efficiently knock-down ARID1A and SNF5 expression and the expression of CTGF in ARID1a- or SNF5-depleted cells

was greatly increased compared to siRNA control-treated cells. As positive control, siRNA against LATS induced CTGF expression 4 times more than siRNA control. The same results were also obtained by depletion of the catalytic ATPase subunits of SWI/SNF complex, BRG1 and BRM (**Figure 6D-F**). The results above suggest that SWI/SNF complex might work as YAP/TAZ inhibitors inside the nucleus. We confirmed the previous observations also by using the synthetic TEAD-dependent luciferase reporter (8xGTIIC-Lux) in HEK293 cells. HEK293 cells were plated in sparse conditions, transfected with siRNAs and 24h later with 8xGTIIC-Lux and CMV-LacZ (to normalize for transfection efficiency). Cells were then harvested 48 hours after DNA transfection. Indeed, we found that depletion of ARID1a or BRM dramatically increased the expression of the reporter compared to siRNA control-treated cells. Moreover, in both conditions, this was YAP/TAZ dependent, as depletion of YAP/TAZ in ARID1A-depleted and BRM-depleted cells abolished the above described induction (**Figure 7**).

YAP interacts with SWI/SNF complex

We wanted to repeat and validate the YAP-SWI/SNF protein-protein interactions previously detected by MS. To do so, we carried out co-immunoprecipitations of overexpressed YAP and individual SWI/SNF components upon co-transfection in HEK293T cells. For these assays, we decided to use HA-YAP 5SA, a YAP mutant for the LATS phosphorylation sites that favors YAP nuclear localization and that was originally used in the MS experiment. As shown in **Figure 8A and 8B**, we coprecipitated HA-YAP 5SA by pulling down Flag-tagged BRM or BRG1. As a control, transfected BRM or BRG1 retain their capacity to bind endogenous BAF53a, ruling out the possibility of artifacts due to these overexpression experiments.

BRG1 and BRM have been previously shown to bind nuclear actin-like molecules also known as BAF53a through a specific domain, called HSA domain. To test the involvement of this domain in the YAP/SWI-SNF interaction we

prepared a Flag-tagged HSA-deletion construct of BRG1 and repeated the coimmunoprecipitation experiments with YAP. As shown in **Figure 8B** lanes 5 and 6, HA-YAP-5SA retained the ability to bind Flag-BRG1-ΔHSA indicating that this domain is dispensable for YAP/BRG recognition. As control of this deletion construct, only wild-type BRG1, but not HSA-deleted BRG1, interacted with BAF53a.

Then, in order to exclude that the YAP/BRG1 interaction was specific of our experimental set up, we repeated the YAP-SWI/SNF interaction by using a distinct IP set up and different cellular context. For this, we employed the mammary immortalized cell line MCF10A stably transduced with Flag-YAP-5SA. Cell lysates from these cultures were used to first precipitate YAP (by using anti-Flag pull down) and then the presence of coprecipitating endogenous SWI/SNF proteins were monitored by western blotting. Indeed, Flag-YAP-5SA coprecipitated endogenous SWI/SNF proteins, including BRG1, BRM ARID1a and SNF5 (**Figure 8C**).

Finally we sought to verify if these associations could occur in a completely endogenous set-up. SWI/SNF is a large protein complex made of several core subunits (BRG1, BRM and ARID1a) and some facultative components (SMARCC1, BAF53a and SNF5). We sought to identify which of these SWI/SNF component(s) is directly binding to YAP. For this, we purchased commercial antibodies against: ARID1a, BRG1, BRM, SMARCC1, BAF53a and SNF5. We found that purification of BRG1 or SMARCC1 triggers co-precipitation of all the other SWI/SNF subunits (For BRG1 pull-down we could identify SMARCC1, BAF53a and SNF5; For SMARCC1 pull-down we could identify BRG1, BAF53a and SNF5) with the exception of ARID1a and YAP. By using SNF5 antibodies, we could co-precititate SMARCC1 but none of the other components. This suggests that SWI/SNF may be heterogeneous in their molecular composition or that antibodies used to precipitate the complex may actually interfere with

complex assembly. Most importantly, when we precipitated the SWI/SNF complex with ARID1a we were able to detect coprecipitation of all the other endogenous components (including BRG1, SMARCC1, BAF53a and SNF5) and also coprecipitation of YAP. These results suggest that YAP association to SWI/SNF occurs only in ARID1a-containing SWI/SNF complexes (**Figure 8D**). Taken together, the data support the notion that YAP interacts with SWI/SNF complex.

YAP directly binds to ARID1a.

The above results raised the possibility that ARID1a may be proximal or directly mediate YAP association to SWI/SNF protein complex. If so, then, depleting cells of the other SWI/SNF subunits should not affect the ARID1a/YAP association. To test this hypothesis, MCF10A cells were transfected with independent siRNAs against BRG1 and BRM. By using these BRG1 and BRM-depleted lysates, we found that endogenous YAP/ARID1a interaction remained well-detectable (**Figure 9A**, lanes 5 and 6) in a way that is comparable to co-IPs from lysates of siRNA-control transfected cells (**Figure 9A**, lanes 3 and 4). As control, knockdown of BRG1/BRM disabled the ability of ARID1a to complex with BAF53a, a finding in line with the published literature that BAF53a directly binds BRG1/BRM, and only indirectly to ARID1a (Szerlong et al., 2008). In other words, our findings suggest that YAP is more likely to directly bind ARID1a, and that ARID1a serves as a link between YAP and the rest of the SWI/SNF complex. To further prove this hypothesis, we knocked down ARID1a and test the effects of this depletion on a BRG1-YAP co-IP. As shown in **Figure 9B,** loss of ARID1a impairs BRG1-YAP interaction (lanes 5 and 6). In contrast knockdown of other SWI/SNF subunits, such as BAF53a and SNF5, had no effect on BRG1-YAP interaction. The data described above indicate that ARID1a is a bridge for the association between YAP and SWI/SNF complex.

YAP binds to ARID1a through its WW domain.

The data presented so far indicates that YAP binds to SWI/SNF likely through ARID1a. With this background in mind, we decided to investigate which domain of YAP is directly involved in ARID1a binding. YAP display different domains, including PDZ Binding motif, TAD (Transcription Activation Domain), Coiled-Coil Domain, WW domain, TEAD Interacting Domain, and a number of YAP interactors have been demonstrated to bind YAP in different domains (**Figure 10A**) (Oren, 2013)(Piccolo et al., 2014). In order to find the exact domain of YAP involved in YAP binding to SWI/SNF protein complex, we carried out structure-function studies in HEK293T cells between overexpressed YAP and endogenous proteins. For this, we prepared C-terminus deletion constructs of Flag-YAP that progressively eliminate from YAP protein sequence three of its domains, that are the PDZ, the TAD and the WW domains (**Figure 10B**). HEK293T cells were then transfected with the indicated YAP deletion constructs and protein extracts were subjected to anti-Flag IP and analyzed for coprecipitating endogenous ARID1a, BRG1 and SNF5. As shown in **Figure 10C**, these SWI/SNF proteins strongly associated to Flag-YAP-ΔPDZ+ΔTAD but not Flag-YAP-ΔPDZ+ΔTAD+ΔWW. This implies that SWI/SNF complex might bind to YAP WW domain. As controls of the previuos IP experiments, YAP/AMOT and YAP/PTPN14 associations were lost after deletion of the YAP WW domain, whereas YAP interaction with TEAD4, reported to happen through the N-terminus part of YAP and independently of the WW domain, was present in all the deletion constructs of YAP here analyzed.

To strengthen these data, we obtained another YAP construct that is mutated only in the WW domain (Tryptophan 258 to Alanine; Proline 261 to Alanine) and found that, compared to wt, YAP WW mut interaction with ARID1a and SNF5 (as well as with AMOT and PTPN14) were completely lost. In contrast, YAP WW mut could still precipitate TEAD4, ruling out the possibility that WW mutation could compromise YAP structure and the general possibility of YAP to

interact with other proteins (**Figure 10D**). Of note, YAP/TEAD interaction is impaired only if the Serine 94 of YAP, specific for TEAD binding (Zhao et al., 2008), is mutated to Alanine.

In conclusion, we have demonstrated that YAP binds to SWI/SNF protein complex, more likely through interaction with ARID1a, and that YAP WW domain is required for this interaction.

F-actin binds to SWI/SNF complex

We next decided to evaluate the interaction between Actin and the SWI/SNF complex in our cellular models. This interaction has been previously documented for BRG1 and in particular the HSA domain of BRG1 was found to be important. (Zhao et al., 1998, Rando et al., 2002 and Szerlong et al., 2008). As Actin is present in the cell mainly as G- (monomeric) or F-(polymerized) actin, we decided to analyze these two pools and their interaction capacity with SWI/SNF complex. In the usual conditions for immunoprecipitation (high detergents in the buffer, high salt concentration, without ATP providing energy, low temperature), formation of G-actin is favored and BRG1 failed to interact with actin. We also optimize the experimental conditions that favor F-actin stabilization and analysis from cell lysates. For this, we used biotinilated-phalloidin (Bio-Phall), a reagent that can stabilize F-actin and that enables us to selectively precipitate F-actin and F-actin-interacting proteins with a streptavidin resin (**Figure 11A**). In the F-actin pull-down assay with Bio-Phall, we could precipitate the SWI/SNF protein complex components ARID1a, BRG1, SMARCC1, SNF5, BAF53a and gelsolin, a known F-actin-interacting protein (positive control) (Szerlong et al., 2008). Lysates from LatA-treated cells were used as negative control. Indeed, by inducing F-actin disassembly, LatA impedes Bio-Phall integration in F-actin fibers, and, as such any pull-down (**Figure 11B**). These results demonstrate that SWI/SNF protein complex can associate with F-actin.

F-actin binding to SWI/SNF cause YAP to dissociate from SWI/SNF

Our findings present the evidence that YAP directly binds to SWI/SNF complexes and F-actin is associated to SWI/SNF complexes. Then, we decided to investigate the relationship between SWI/SNF, F-actin and YAP. To address this point, we employed co-immunoprecipitation assays to pull down endogenous YAP in MII cells treated with either Lat.A (i.e. NO F-actin) or phalloidin (i.e., PLUS F-actin), and we then checked by western bolt the coprecipition of SWI/SNF protein complex components. As shown in the **Figure 11C**, in the presence of intact F-actin (with Phalloidin), the endogenous YAP-SWI/SNF association was absent (lane 4): however, upon disruption of F-actin cytoskeleton (with Latrunculin A), YAP-SWI/SNF association became evident (lane 3). The result above suggests a model for the regulation of the nuclear activity of YAP by F-actin: when cells are highly packed or plated on a soft ECM, the F-actin cytoskeleton is disrupted and YAP is inhibited by SWI/SNF complex; when cells are cultured at low confluence or on a stiff ECM, F-actin is activated and YAP is released from SWI/SNF complex. We found before that ARID1a was the bridge between YAP and SWI/SNF complex. Therefore, we want to further test if ARID1a was still important in mechanical regulated YAP-SWI/SNF association. To do so, we repeated the endogenous YAP immunoprecipition in extracts from LatA-treated cells in the presence or absence of ARID1A to check how these conditions affect YAP interactors. Upon ARID1a depletion, the interaction between YAP and the SWI/SNF protein components BRG1, SMARCC1, and SNF5 was abolished in Lat.A-treated cells (**Figure 11D**, lane 5 and 6).

The data presented so far provide strong biochemical evidence that YAP could interact with SWI/SNF only when F-actin is not associated to the SWI/SNF complex.

Knockdown of ARID1a rescue YAP activity from mechanical regulation

We have demonstrated that YAP directly binds to SWI/SNF protein complex, and we hypothesized that this represented an inhibitor regulation of YAP (**Figure 8-11**). According to this model, if we induce the depletion of the SWI/SNF complex, we should restore YAP/TAZ activity in mechanically-inhibited cells (cells plated at high density or on soft ECM). Since knockdown of ARID1a could not affect YAP/TAZ localization in high confluent cells (data not shown), we decided to use LMB to relocate YAP/TAZ into nucleus. We previously showed that even if YAP/TAZ were nuclear because of LMB treatment, YAP/TAZ were inactive in densely packed cells (**Figure 3**). As we found that ARID1A is a mechano-sensitive nuclear inhibitor of YAP/TAZ, we indeed argued that depletion of ARID1A could rescue the previous transcriptional inhibition of YAP. To test this hypothesis MCF10A cells were first transfected with two independent siRNAs against ARID1A; next cells were replated at high density in the presence or absence of LMB; then cells were harvested for qPCR analysis (**Figure 12A**). Indeed, upon ARID1A depletion, highly-confluent MCF10A cells treated with LMB rescued CTGF and CYR61 expression (**Figure 12B and 12C**).

Next, we repeated the experiment in soft ECM. MCF10A cells were transfected with two independent siRNAs against ARID1a. The day after transfection, cells were replated as single cells on soft hydrogel (0.7 KPa, soft ECM) and, 24 hours after replating, cells were harvested for qPCR analysis. As before, the CTGF and PTX3 expression was restored only after depletion of ARID1A (**Figure 12D and 12E**).

In conclusion, the inhibition of the transcriptional activity of YAP/TAZ caused by mechanical regulation can be rescued by ARID1a depletion.

SWI/SNF complexes work as YAP inhibitors in Neurons

Next, we wanted to find out the biological relevance of YAP-SWI/SNF interaction. YAP is known for its powerful function of growth and tumor

promoter. In order to find out the function of SWI/SNF complexes in YAP-regulated cell growth, we knockdown the core components of SWI/SNF, such as ARID1a, BRG1, BRM or SNF5, and test their influence on BrdU incorporation in multiple cell lines: however, we found that loss of SWI/SNF component barely change the cell proliferation (data not shown). This result put us in the corner and left no option to study SWI/SNF role in YAP-involved tumorigenesis. It is broadly accept that two events are very important during tumor formation. Aberrant proliferation is for sure important and considered an hallmark of cancer, but data from different types of human cancers and mouse models at least suggest that acquisition of an immature, stem-like status by differentiated cells is a prerequisite for tumor progression. This process is known as dedifferentiation. In the ongoing work of our laboratory, we found that transient YAP overexpression could reprogram fully differentiated cells back to their progenitor cells: this is remarkably true for example in neurons, which can be convert to neural stem cells by transient YAP expression. As we identified SWI/SNF proteins as inhibitors of YAP/TAZ, we decided to test whether YAP-induced neuron-to-NSC dedifferentiation was enhanced by loss of SWI/SNF. Following this idea we performed the experiment shown in **Figure 13A**. Hippocampal neurons were derived from late embryos and plated on poly-L-lysine pre-coated cell culture plates. Then we first infected neurons with tetO-YAP and rtTA-encoding lentiviruses, and selected for mature neurons by culturing them in neuronal medium containing the anti-mitotic drug AraC. After selection, neurons were infected with shRNA vectors against either BRM or ARID1a (knockdown efficiencies were checked in **Figure 13D**). YAP expression was then induced in these cultures by addition of doxycycline in NSC medium. Within 15 days of YAP overexpression, neurons lost their morphology and were converted to NSC-like cells able to form spherical colonies. As shown in the **Figure 13B**, concomitant knockdown of ARID1a or BRM by shRNA could remarkably increase YAP-induced dedifferentiation compare to shRNA control (quantifications see **Figure 13C**) as measured by the increase in the number of

initiating spheres. The results showed above imply that SWI/SNF complex works as a barrier during YAP-induced reprograming.

Loss of SWI/SNF complex could help YAP to overcome mechanoregulation

We next want to investigate if YAP-induced reprogramming of neurons to a NSC-like cells was regulated by mechanotransduction through SWI/SNF. To answer this question, we plated neurons on top of a Matrigel matrix in order to mimic a soft ECM and treated them as above (**Figure 14A**). Once neurons were plated on soft Matrigel (soft ECM), the YAP-induced reprogramming was impaired with respect to what happens on a stiff ECM (plastic) (**Figure 14B and 14C**): indeed the culture appears as aggregates of neurons expressing the neuronal marker NeuN, whereas, on plastic, neurons are converted to SOX2-expressing cells by transgenic YAP-expression, that confirmed their transition to a neural stem cell-like status (**Figure 16**). In conclusion, we found that the YAP-induced reprogramming of neurons is mechanosensitive and is greatly impaired if neurons are plated on a soft ECM. Remarkably, knockdown of SWI/SNF complex components Arid1a and Brm could help YAP-induced reprogramming to overcome this mechanical regulation (**Figure 15B and 15C**). Indeed, Arid1a- or Brm-depleted neurons greatly shift to a NSC-like status, as, even if plated on top of a soft ECM, they start to form spherical aggregates expressing the neural stem cell marker SOX2 (**Figure 16**).

In conclusion, i) SWI/SNF complexes work as negative regulators during YAP-induced reprogramming of neurons. ii) Mechanical regulation could impair YAP-induced reprogramming. iii) Depletion of SWI/SNF could release YAP from mechanical regulation.

DISCUSSION

The data described here presents several elements of novelty.

1) Nuclear localization of YAP/TAZ does not translate into YAP/TAZ activity: need of intra-nuclear activation to turn on YAP/TAZ-dependent transcription

It is generally accepted that YAP/TAZ localization by immunofluorescence represents a proxy of their activity. In light of the data here presented, we propose that nuclear localization is an obvious prelude to activity, but not a proof of it. Indeed, when we enforced YAP/TAZ nuclear localization by LMB, YAP/TAZ transcription activity was still inhibited in cells experiencing low mechanical cues (such as cells seeded in high confluence or on soft ECM) (**Figure 2-4**). This indicates that mechanotransduction does not end with cytoplasmic F-actin tension and organization, but also entails a nuclear step. In other words, different mechanosensitive "layers" may exist in cells: some are cytoplasmic and connected to organization of the F-actin. An anti-YAP cytoskeleton would include an F-actin organization that is very dynamic, generating short fragments by the activity of severing proteins and mainly structured as cortical actin layer. Oppositely, a cytoplasmic F-actin organization as stress fibers, and actin association to focal adhesion and actomyosin contractility represent a pro-YAP conditions. A shift from a cytoskeleton that corresponds to a mechanically soft to a stiff condition can be induced by attenuation of F-actin regulators, such as cofillin, gelsolin and CapZ (Aragona et al., 2013). Yet, even in these conditions nuclear mechanotransduction must also occur and entail F-actin regulation of SWI/SNF.

Nuclear F-actin. Actin is a very abundant protein in the cytosol of mammalian cells, but can be also found in the nucleus. In this location, its

concentration is lower and confounded by classic cell biology experiments by the cytoplasmic staining, which complicates the investigation of its nuclear functions. In addition, the control of nuclear actin dynamics is very complex as most actin regulators undergo nucleocytoplasmic shuttling in a highly dynamic manner. Actin itself is imported and exported by importin 9 and exportin 6 (Dopie et al., 2012; Stüven et al., 2003). Thus, modulation of nuclear actin is dictated in non-obvious ways by F-actin mechanics and organization in the cytoplasm, and from availability and shuttling dynamics of its regulators. It is therefore not surprising that the formation of nuclear filamentous actin (F-actin) has been controversial, up to the point that nuclear actin was considered to be entirely or mainly monomeric in its nature. However, several groups demonstrated the existence of nuclear F-actin structures in somatic cell nuclei using actin probes of high sensitivity ("life-Act"-GFP)(Baarlink et al., 2013; Navarro-Lérida et al., 2015). It appears that cells possess a rich, extremely dynamic network of F-actin and that this can be regulated by serum (a known potent inducer of F-actin polymerization in the cytoplasm)(Baarlink et al., 2013) or upon cell spreading on a substrate(Plessner et al., 2015). In other words there is a continuum between ECM organization and extracellular tension, integrin receptor, cytoplasmic F-actin and then nuclear F-actin, perhaps connected through the LINC complex, a components of the nuclear lamina bridging the cytoskeleton with the nucleoskeleton. Clearly, this cascade, through details that remain to be determined, reach YAP/TAZ activity in the nucleus, stabilizing its function.

2) SWI/SNF link nuclear F-actin to YAP/TAZ function.

In this study, we demonstrated that SWI/SNF complexes bind to YAP through YAP WW domain. (Skibinski et al., 2014) suggested already a physical association between BRG1 and TAZ. Our studies instead indicate that YAP is directly binding to ARID1a but not BRG1 (**Figure 9**). We thus respectfully

suggest that what (Skibinski et al., 2014) were detecting was an indirect association between BRG1 and TAZ, likely mediated by ARID1a. Alternatively, it is also possible that YAP and TAZ may associate to the SWI/SNF complex through distinct mechanisms. In most assays, in fact, YAP and TAZ are functionally identical and typically redundant with each other by loss-of-function. That said, they are also highly related but not absolutely identical proteins and their individual germ-line knockout phenotype at least indicate an earlier and more profound, essential requirement of YAP during embryogenesis. This is to say that it might not be surprising that YAP/TAZ would display different mechanisms of regulation.

An important discovery here is that SWI/SNF complexes are YAP/TAZ inhibitors inside the nucleus (**Figure 6 and 7**). This was shown first in cell lines, using MCF10A and HEK293 cells. Loss of SWI/SNF components in these cells causes increased activity of YAP/TAZ endogenous targets and luciferase TEAD/YAP/TAZ-artificial sensors. This indicated that SWI/SNF are buffering YAP/TAZ activity.

This discovery represents a novelty in the epigenetic field. SWI/SNF are in textbooks of molecular biology because of their ability to mobilize nucleosomes and remodel chromatin by utilizing the energy of ATP hydrolysis (Kassabov et al., 2003; Phelan et al., 1999). These 2 MDa complexes are made up of 12–15 subunits. Some core subunits are present in all SWI/SNF complexes, including SNF5 (or SMARCB1/INI1/BAF47), SMARCC1 (BAF155) one of the catalytic ATPase subunit, either BRG1 (SMARCA4) or BRM (SMARCA2). In addition, there are subunits present only in some variants, such as ARID1A and ARID1B, that are mutually exclusive subunits for BAF complexes, and PBRM1 and ARID2, specific for PBAF complexes (**Figure 1A**) (Wang et al., 1996; Wu et al., 2009).

Here we found that ARID1a serves as bridge between YAP and SWI/SNF. In preliminary results not shown here, we failed to detect similar functions by

ARID1b, limiting the possibility of a functional redundancy. The composition of SWI/SNF complexes in time, space and cell type is a mystery. In light of the rather specific role of ARID1a as YAP inhibitor, ARID1a function as leading tumor suppressor and of the role of YAP during cancer and tissue repair, it would be tempting to propose that ARID1a may be a facultative components recruited to SWI/SNF complexes under some form of tissue stress or when tissues need to cope with rapid growth.

3) A mechanisms for SWI/SNF tumor suppressive effects

As introduced, 20% of all human tumors present inactivating mutations in SWI/SNF components. ARID1a is particularly prominent in these lists being mutated (loss of function) in 45% of ovarian clear cell and endometrioid carcinomas (Jones et al., 2010); 19% of bladder cancers; 19% of gastric cancers; 14% of hepatocellular cancers; 12% of melanomas; and also less frequently in lung, breast, colorectal, pancreas, and several other types of cancer (summarized in (Helming et al., 2014)). The function of mutated SWI/SNF complexes in cancer and the mechanisms by which mutations in individual subunits promote oncogenesis are now active areas of research.

When we initiated these studies, our first assays for SWI/SNF have been cell proliferation assays. Overall we got disappointing results: loss of SWI/SNF is either detrimental for cell survival or dispensable. This is apparently at odd with their role as tumor suppression, but in line with their well-established and fundamental determinants of chromatin biology. Clearly the sophistication of SWI/SNF composition (presence or absence of facultative components, also keeping in mind that BRG1 and BRM are invariably kept as separate entities) allows cells to display a great plasticity: the possibility to use one subtype for one fundamental function (i.e. nucleosome remodeling) and the other for other, perhaps more sophisticated and unknown tumor suppressing functions. In turn "tumor suppression" is word for a generic concept not automatically connected to

the control of cell proliferation. In several cell lines, we were initially discouraged by finding that ARID1a inactivation was actually inconsequential for cell proliferation (by BrDU incorporation and Ki67 stainings). This prompted us to search for a function of ARID1a connected to different functions of YAP/TAZ also unrelated to cell growth *per se*. Instead, our data seem to suggest that SWI/SNF are tumor suppressors because they inhibit YAP/TAZ-induced cell dedifferentiation. Thus growth and dedifferentiation represent different entities, potentially controlled by different SWI/SNF complex. See point 4 of this discussion.

Future perspective. To gain insight this problem, for the future, we plan to carry out in vivo experiments using established mouse models either of tumorigenesis or dedifferentiation. To test whether YAP/TAZ activity is in fact downstream of SWI/SNF inactivation, we will cross LOX-STOP-LOX KRasG12V; Arid1a -/+ mice, with YAP/TAZ conditional alleles under the control of the K14-CreERT2 and K8-CreERT2 drivers, mediating deletion in the basal and luminal compartments of the mammary gland, respectively (van Keymeulen et al, 2015). With these experiments, we will test if loss of YAP/TAZ (in either compartments) rescues tumor suppression in the ARID1a mutant background; or if their loss in already established, fully grown mammary gland tumors (by timing tamoxifen addition) enhances their differentiation (as monitored by histology and/or FACS profile), and is accompanied by the loss of prospective cancer SCs (as validated by the mammosphere self-renewal assay). In a complementary approach, we will address the requirement of SWI/SNF complexes for YAP/TAZ dependent acquisition of cancer SC properties by non-CSCs. For this, we will evaluate the acquisition of self-renewal and tumorigenic potential of mammary cells after TAZ overexpression (or endogenous TAZ activation by EMT) and depletion of ARID1a, BRG1 and/or BRM.

4) YAP/TAZ induced reprogramming is regulated by mechanical cues.

In an independent research line of our lab, we found that ectopic expression of YAP in terminally differentiated cells, such as primary neurons, can trigger their dedifferentiation and acquisition of stem cells traits (this work is currently submitted as Panciera et al.). In this thesis, we took advantage of these studies and used YAP-induced cell dedifferentiation of neurons into NSCs as a playground to study: A) the role of mechanical signals as essential for cell reprogramming and somatic SC acquisition, demonstrating that a pliant, soft ECM microenvironment preserves cell differentiation, blunting the effect of YAP overexpression; and B) the role of ARID1a (and Swi/SNF more in general) as factors involved in preserving cell differentiation on pliant ECMs. Mechanistically, this is mediated by SWI/SNF serving as a mechanosensors: the complex indeed seems to bind to YAP through the ARID1a bridge in soft cells and in a mutually exclusive manner to F-actin. In soft and stiff cells SWI/SNF complex thus appear to change its composition: from a SWI/SNF/ARID1a-YAP/TAZ in soft cells to a SWI/SNF/F-actin in stiff cells. In soft cells, a SWI/SNF/ARID1a-YAP/TAZ complex prevents YAP/TAZ activity on target in primary cells. This gatekeeper function is surpassed once the complex switches to a SWI/SNF/F-actin mode, setting free YAP and as such unleashing its de-differentiation and, at least in cancer, tumor progressive functions. Our results have thus far reaching implications. Finding that a transient exposure to YAP and TAZ is sufficient to rewire the genome of fully differentiated cells into multipotent SC-like cells bears profound implications for cancer biology. Cancer is a disease of disturbed cell differentiation as much as it is of aberrant cell proliferation. In the past 30 years, emphasis has been placed on oncogenic regulation of tumor growth (Hanahan and Weinberg, 2011). Data from different types of human cancer and mouse models at least suggest that acquisition of an immature, stem-like state is a prerequisite for tumor progression(Hanahan and Weinberg, 2011). This issue obviously connects with another fundamental question, that is, what is the cancer cell of origin. In one scenario, oncogenes may hit normal tissue SCs that already possess the self-renewal and differentiation capacities normally used for tissue replenishment.

An alternative (although not mutually exclusive) scenario is that tumor cells may be generated *de novo* from more differentiated healthy/normal cells. Indeed, activation of RasG12V combined with loss-of-p53 has been shown to readily reprogram terminally differentiated neurons into glioma-SCs (Friedmann-Morvinski et al., 2012); and RasG12V combined with loss-of-APC induced differentiated intestinal cells to become tumor initiating cells (Schwitalla et al., 2013). It is thus possible that, at their incipit, oncogenic lesions may first promote the generation of de-differentiated cellular states that are permissive for proliferation and self-renewal. In vivo, cells emerging from this oncogene-mediated reprogramming may be restrained by the normal tissue context. The persistence of this state coupled with other genetic, epigenetic and environmental alterations such as a raise in the architecture or rigidity of the environement may allow a second phenotypic switch, that is, transition to a tumor initiating cell whose self-renewal has become unresponsive to the tumor suppressive tissue context.

Future perspectives. Tumor progression is frequently accompanied by an increase in stem cell representation (Di Fiore Pece) within the tumor, by ARID1a mutations and by a raise in YAP/TAZ activity. As discussed above, our results provide a mechanism that connected these events. It will be now important to test whether loss of ARID1a causes breast cancer cells to switch to a more undifferentiated cancer-stem-cell-like status, phenocopying earlier results obtained with TAZ or YAP overexpression.

It will be also important to test whether somatic cell reprogramming induced by expression of ectopic YAP/TAZ does reflect in a similar relevance of endogenous YAP/TAZ during dedifferentiation occurring in vivo during tumorigenesis induced in neurons by common oncogenic lesions such as PDGF overexpression, loss of p53 or activation of Ras mutations. It will be important to combine this with mouse mutants for YAP/TAZ to test if these events are

addicted to YAP/TAZ and whether a sufficient cell mechanics is involved and permissive for dedifferentiation to a somatic SC status by cancer cells.

EXPERIMENTAL PROCEDURES

Reagents and plasmids

Latrunculin A, Leptomycin B and phalloidin were from Sigma. Doxycycline was from Calbiochem. Matrigel was from BD.

pCDNA3 FLAG-hYAP1 WT and FLAG-hYAP1 5SA were generated by PCR from original HA-tagged cDNAs kindly provided by Dr. Guan, made insensitive to YAP siRNA#1 and siRNA#2 by point mutagenesis (Dupont et al., 2011) and subcloned in pBABE retroviral plasmids to establish stable cell-lines. pBABE-Hygro empty vector was used as control retroviral transduction. For YAP structure function studies of **Figure 10**, deletion constructs of Flag-hYAP1 were generated by PCR. Flag-YAP WW mut were introduced mutations (Tryptophan 258 to Alanine and Proline 261 to Alanine) into pCDNA3 FLAG-hYAP1. Flag-YAP S94A was generated by site-specific PCR mutagenesis. For inducible expression in mouse neurons, YAP WT was subcloned in a doxycycline-inducible lentiviral expression vector (Fu-tetON, Cordenonsi et al, 2011). The 8xGTIIC-lux (Dupont et al., 2011) is (Addgene #34615). pCS2 Flag-BRM was obtained by subcloning Flag-BRM from pBABEpuro Flag-BRM (Addgene #1961) into pCS2. pCS2 Flag-BRG1 was obtained by subcloning Flag-BRG1 from pBABEpuro Flag-BRG1 (Addgene #1957) into pCS2; Flag-BRG1 ΔHSA was generated by PCR by deleting HSA domain (deletion of residues 462-532). The constructs for shControl, shArid1a, and shBrm expression in primary neurons were prepared by cloning the Control, mouse siARID1A#1, mouse siARID1A#2, mouse siBRM#1 and mouse siBRM#2 sequences (see RNAi section) into pLKO.1-puro lentiviral vector (Addgene #8453;Stewart et al. 2003)) according to manufacturer's protocol.

All constructs were confirmed by sequencing.

Cell lines and treatments

MII cells were a gift from S. Santner (Santner et al., 2001). MCF10A and MII cells were cultured in DMEM/F12 (Gibco, Life Technologies) with 5% horse serum (HS), glutamine and antibiotics, freshly supplemented with insulin, EGF, hydrocortisone, and cholera toxin. HEK293 and HEK293T cells were cultured in DMEM (Gibco, Life Technologies) supplemented with 10% fetal bovine serum (FBS), glutamine and antibiotics.

Cells plated on plastic are considered as cultured on a stiff ECM. For experiments on soft ECM, 5,000–10,000 cells per cm2 were seeded in drop on top of 0.7 kPa hydrogels; after attachment, the wells containing the hydrogels were filled with appropriate medium. Cells were then harvested for immunofluorescence or RNA extraction after 24 hours. For experiments with higly confluent cells, we plated 200000 cells per cm2 in the appropriate well; after attachment, the wells filled with medium. Cells were then harvested for immunofluorescence or RNA extraction after 24 hours.

Latrunculin A was used at a final concentration of 0.5 μM for the time indicated in the text. LMB was incubated at a final concentration of 15 ng/ml for the last two hours of the indicated experiments.

RNA interference

siRNA transfections were done with Lipofectamine RNAi-MAX (Life technologies) in antibiotics-free medium according to manufacturer instructions. Sequences of siRNAs are provided in **Table 3**.

Western blot

Cells were harvested by sonication and extracts quantified with Bradford

method. Proteins were run in 4-12% Nupage-MOPS acrylamide gels and transferred onto PVDF membranes by wet electrophoretic transfer. Blots were blocked with non-fat dry milk and incubated overnight at 4°C with primary antibodies. Secondary antibodies were incubated 1 hr at room temperature, and then blots were developed with chemiluminescent reagents. Images were acquired with Image Quant LAS 4000 (GE healthcare).

For Western blot: anti-YAP/TAZ, anti-BAF53a, anti-BRG1, anti-SMARCC1, anti-PTPN14, anti-TEAD4, anti-AMOT, anti-Gelsolin (GSN) were from Santa Cruz. anti-LATS1 was from CST. anti-ARID1A and anti-SNF5 were Sigma. anti-YAP and anti-BRM were from Abcam. anti-TEAD1 was from BD. anti-Actin was from Cytoskeleton. anti-GAPDH monoclonal antibody was from Millipore. Horseradish-peroxidase-conjugated anti-Flag (clone M2, A8592) was from Sigma and the anti-HA (A190-107P) was from Bethyl.

Luciferase Assays

Luciferase assays were performed in HEK293 cells with the established YAP/TAZ-responsive luciferase reporter 8xGTIIC-Lux (Dupont et al., 2011). 8xGTIIC-Lux reporter (50 ng/cm^2) were transfected together with CMV-β-gal (75 ng/cm^2) to normalize for transfection efficiency with CPRG (Roche) colorimetic assay. DNA transfections were done with TransitLT1 (Mirus Bio) according to manufacturer instructions. DNA content in all samples was kept uniform by adding pBluescript plasmid up to 250 ng/cm^2. In experiments in siRNA-depleted cells (**Figure 7**), cells were first transfected with the indicated siRNAs and, the day after, washed from transfection media, transfected with plasmid DNA, and harvested 48 hr later. Each sample was transfected in duplicate and each experiment was repeated at least three times independently.

Quantitative Real-Time PCR

Cells were harvested by RNeasy Mini Kit (Quiagen) for total RNA extraction, and contaminant DNA was removed by DNase treatment. qRT-PCR analyses were carried out on retrotranscribed cDNAs with Rotor-Gene Q thermal cycler (Quiagen) and analyzed with Rotor-Gene Analysis 6.1 software. Experiments were performed at least three times, with duplicate replicates. Expression levels are always given relative to GAPDH. PCR oligo sequences are listed in **Table 1**.

F-actin pulldown

For the experiments depicted in **Figure 11B**, cells were plated in sparse conditions and either left untreated or treated for 4 hours with Lat.A (LatA for this sample condition was kept also in the following buffers used for harvesting and immunoprecipitation). Cells were then harvested in Actin lysis buffer (20 mM HEPES (pH 7.8), 50 mM KCl, 0.1% Triton, 5% Glycine, 0.1% NP40, 5 mM $MgCl_2$, 1 μM DTT, MG105/MG132, phosphatase and protease inhibitors) containing Biotinilated-Phalloidin (Sigma) and mechanically disrupted. Extracts were cleared by centrifugation and incubated at room temperature for three hours streptavidin-coniugated resin (Sigma). Phalloidin complexes were then washed with Actin lysis buffer three times at room temperature resuspended in SDS sample buffer, and subjected to SDS-PAGE and Western blot analysis.

Coimmunoprecipitation of Endogenous proteins

For immunoprecipitations of endogenous proteins of **Figures 8D and 9A**, Cells were harvested and lysed by sonication in Lysis Buffer (50 mM HEPES (pH 7.8), 100 mM NaCl, 50 mM KCl, 1% Triton, 5% Glycine, 0.5% NP40, 2 mM $MgCl_2$, 1 μM DTT, phosphatase and protease inhibitors) and cleared by centrifugation.

Extracts were incubated with anti-ARID1A (Santa Cruz) antibody or control rabbit IgG immobilized on Protein G-Sepharose beads at 4°C overnight.

Immunocomplexes were then washed with cold Lysis buffer three times, resuspended in SDS sample buffer, and subjected to SDS-PAGE and Western blot analysis.

For the experiments depicted in **Figures 11C and D**, cells were plated in sparse conditions and treated for 4 hours with either Phalloidin or Lat.A. For Phalloidin-treated samples, Phalloidin was kept also in the following buffers used for harvesting and immunoprecipitation. For Lat.A-treated samples, Lat.A was kept also in the following buffers used for harvesting and immunoprecipitation). Cells were then harvested in Actin lysis buffer and mechanically disrupted. Extracts were cleared by centrifugation and incubated with anti-YAP (Abcam) antibody or control rabbit IgG immobilized on Protein G-Sepharose beads at 4°C overnight. Immunocomplexes were then washed with Actin lysis buffer three times, resuspended in SDS sample buffer, and subjected to SDS-PAGE and Western blot analysis.

Coimmunoprecipitation of Tagged proteins

Cells were transfected with the indicated plasmids; after 48 hours, cells were harvested and lysed by sonication in Lysis Buffer (50 mM HEPES (pH 7.8), 100 mM NaCl, 50 mM KCl, 1% Triton, 5% Glycine, 0.5% NP40, 2 mM $MgCl_2$, 1 μM DTT, phosphatase and protease inhibitors). Extracts were incubated three hours at 4°C with anti-Flag resin (Sigma). Immunocomplexes were then washed with cold Lysis buffer three times, resuspended in SDS sample buffer, and subjected to SDS-PAGE and Western blot analysis. Inputs were loaded according to Bradford.

Mass Spectroscopy

Eluates from immunoprecipitations described in **Figure 5** were run in a 4-12% gradient SDS-Page acrylamide gel and the gel was sent to the EMBL core proteomic facility for MS analysis. Each sample lane was cut into five pieces

according to molecular weight, and all the proteins contained in each piece subjected to in-gel tryptic digestion. The resulting peptides were purified and subjected to identification based on their mass according to EMBL parameters.

Immunofluorescence

Cells were fixed 10 min at room temperature (RT) with PFA 4%. Slides were permeabilized 10 min at RT with PBS 0.3% Triton X-100, and processed for immunofluorescence according to the following conditions: blocking in Goat Serum (GS, 10%) in PBST for 1.5 hr, followed by incubation with primary antibodies (diluted in 2% GS in PBST) for 16 hr at 4°C, four washes in PBST and incubation with secondary antibodies (diluted in 2% GS in PBST) for 1.5 hr at room temperature. After three washes in PBS, nuclei were stained with ProLong DAPI (Life Technologies). Primary antibodies are: anti-YAP/TAZ (Santa Cruz), anti-NeuN (Abcam), anti-SOX2 (CST). Secondary antibodies (1:200; Invitrogen) are: goat anti-mouse Alexa568, goat anti-rabbit Alexa488, goat anti-mouse647. When indicated, Alexa488-conjugated phalloidin (Life Technologies) was used 1:200 during secondary antibodies incubation to visualize F-actin microfilaments. Confocal images were obtained with a Leica TCS SP5 equipped with a CCD camera.

Immunofluorescence on matrigel

Cells were fixed with 4% PFA at room temperature for 24 h. The fixed cells were then permeabilized with PBS 0.3% Triton X-100 and blocked by incubating with a blocking solution containing 50 mM Tris (pH7.4), 0.1% Tween-20, 10% GS, 1% BSA, and 0.3 M glycine at 4°C for 12 h. After washing with TBS containing 0.1% (v/v) Triton X-100 (TBST), the 3D cultures were incubated with primary antibodies in the blocking solution at 4°C for 24 h. After washing five times with TBST (each time 1 hour at 4 °C), cells were further incubated with AlexaFluor secondary antibodies (LifeTechnologies) overnight at 4 °C. After

three washes in TBST, nuclei were stained with ProLong DAPI (Life Technologies). Confocal images were obtained with a Leica TCS SP5equipped with a CCD camera.

Lentivirus preparation

HEK293T cells (checked routinely for absence of mycoplasma contaminations) were kept in DMEM supplemented with 10% FBS (Life Technologies), Glutamine and Antibiotics (HEK medium). Lentiviral particles were prepared by transiently transfecting HEK293T with lentiviral vectors (10 micrograms/10 cm dishes) together with packaging vectors pMD2-VSVG (2.5 micrograms) and pPAX2 (7.5 micrograms) by using TransIT-LT1 (Mirus Bio) according to manufacturer instructions.

Primary neuron isolation, infection and culturing

Neurons were prepared from hippocampi of E18-19 wild-type embryos. Briefly, hippocampi were dissected under the microscope in ice cold HBSS as quick as possible, incubated with 0.05% trypsin (Life Technologies) 15 min at 37°C and, after trypsin blocking, resuspended in DMEM/10% FBS supplemented with 0.1 mg/ml DNase I (Roche), and mechanically dissociated by extensive pipetting. Cells were then plated on poly-L-lysine-coated wells (stiff conditions) or on top of a Matrigel layer (soft conditions) in DMEM supplemented with 10% FBS, glutamine and antibiotics for hippocampal neurons, or in DMEM/Neurobasal (1:1) supplemented with 5% FBS, 1x B27, glutamine and antibiotics for cortical neurons (day 1). After 24 hours (day 2), the medium of hippocampal preparation was changed to fresh DMEM/Neurobasal (1:1) supplemented with 5% FBS, 1X B27, glutamine and antibiotics. For reprogramming experiments neurons were infected on the following day (day 3) with FUW-tetO-wtYAP and FUdeltaGW-rtTA viral supernatants. Negative controls were provided by neurons transduced with FUdeltaGW-rtTA alone or in

combination with FUW-tetO-EGFP. After 24 hour (day 4), medium was changed and cells were incubated in Neurobasal medium supplemented with 1X B27, glutamine, antibiotics, and 5 μM Ara-C (cytosine β-D-arabinofuranoside; Sigma) for additional 7 days, at the end of which well-differentiated, complex network-forming neurons are visible. Then, neurons were infected with pLKO.1-shRNA as indicated and negative control was shCO. For this for a typical 3.5 cm plate, we mixed 500 μl of PLKO.1-shRNA produced in NSC medium (DMEM/F12 supplemented with 1X N2, 20 ng/ml murine EGF, 20 ng/ml murine bFGF, glutamine, and antibiotics) and 1.5 ml of serum-free Neurobasal medium with 1X B27. Treated neurons were switched to NSC medium and 2 μg/ml doxycycline for activating tetracycline-inducible gene expression. After 7 days, fresh doxycycline (final concentration of 2 μg/ml) was added. Sphere formation was evident upon YAP induction after 14 days of doxycycline treatment.

REFERENCES

Aragona, M., Panciera, T., Manfrin, A., Giulitti, S., Michielin, F., Elvassore, N., Dupont, S., Piccolo, S., 2013. A mechanical checkpoint controls multicellular growth through YAP/TAZ regulation by actin-processing factors. Cell 154, 1047–59. doi:10.1016/j.cell.2013.07.042

Baarlink, C., Wang, H., Grosse, R., 2013. Nuclear actin network assembly by formins regulates the SRF coactivator MAL. Science 340, 864–7. doi:10.1126/science.1235038

Basu, S., Totty, N.F., Irwin, M.S., Sudol, M., Downward, J., 2003. Akt Phosphorylates the Yes-Associated Protein, YAP, to Induce Interaction with 14-3-3 and Attenuation of p73-Mediated Apoptosis. Mol. Cell 11, 11–23. doi:10.1016/S1097-2765(02)00776-1

Bultman, S., Gebuhr, T., Yee, D., La Mantia, C., Nicholson, J., Gilliam, a, Randazzo, F., Metzger, D., Chambon, P., Crabtree, G., Magnuson, T., 2000. A Brg1 null mutation in the mouse reveals functional differences among mammalian SWI/SNF complexes. Mol. Cell 6, 1287–95.

Cai, J., Zhang, N., Zheng, Y., de Wilde, R.F., Maitra, A., Pan, D., 2010. The Hippo signaling pathway restricts the oncogenic potential of an intestinal regeneration program. Genes Dev. 24, 2383–8. doi:10.1101/gad.1978810

Carlén, M., Meletis, K., Göritz, C., Darsalia, V., Evergren, E., Tanigaki, K., Amendola, M., Barnabé-Heider, F., Yeung, M.S.Y., Naldini, L., Honjo, T., Kokaia, Z., Shupliakov, O., Cassidy, R.M., Lindvall, O., Frisén, J., 2009. Forebrain ependymal cells are Notch-dependent and generate neuroblasts and astrocytes after stroke. Nat. Neurosci. 12, 259–67. doi:10.1038/nn.2268

Chen, C.S., 1997. Geometric Control of Cell Life and Death. Science (80-.). 276, 1425–1428. doi:10.1126/science.276.5317.1425

Coussens, L.M., Werb, Z., 2002. Inflammation and cancer. Nature 420, 860–7. doi:10.1038/nature01322

Da, C.-L., Xin, Y., Zhao, J., Luo, X.-D., 2009. Significance and relationship between Yes-associated protein and survivin expression in gastric carcinoma and precancerous lesions. World J. Gastroenterol. 15, 4055–61.

de la Serna, I.L., Ohkawa, Y., Imbalzano, A.N., 2006. Chromatin remodelling in mammalian differentiation: lessons from ATP-dependent remodellers. Nat. Rev. Genet. 7, 461–73. doi:10.1038/nrg1882

Dopie, J., Skarp, K.-P., Rajakylä, E.K., Tanhuanpää, K., Vartiainen, M.K., 2012. Active maintenance of nuclear actin by importin 9 supports transcription. Proc. Natl. Acad. Sci. U. S. A. 109, E544–52. doi:10.1073/pnas.1118880109

Dupont, S., Morsut, L., Aragona, M., Enzo, E., Giulitti, S., Cordenonsi, M., Zanconato, F., Le Digabel, J., Forcato, M., Bicciato, S., Elvassore, N., Piccolo, S., 2011. Role of YAP/TAZ in mechanotransduction. Nature 474, 179–83. doi:10.1038/nature10137

Dykhuizen, E.C., Hargreaves, D.C., Miller, E.L., Cui, K., Korshunov, A., Kool, M., Pfister, S., Cho, Y.-J., Zhao, K., Crabtree, G.R., 2013. BAF complexes facilitate decatenation of DNA by topoisomerase IIα. Nature 497, 624–7. doi:10.1038/nature12146

Eroglu, E., Burkard, T.R., Jiang, Y., Saini, N., Homem, C.C.F., Reichert, H., Knoblich, J. a, 2014. SWI/SNF complex prevents lineage reversion and induces temporal patterning in neural stem cells. Cell 156, 1259–73. doi:10.1016/j.cell.2014.01.053

Fernández, B.G., Gaspar, P., Brás-Pereira, C., Jezowska, B., Rebelo, S.R., Janody, F., 2011. Actin-Capping Protein and the Hippo pathway regulate F-actin and tissue growth in Drosophila. Development 138, 2337–46. doi:10.1242/dev.063545

Fitamant, J., Kottakis, F., Benhamouche, S., Tian, H.S., Chuvin, N., Parachoniak, C.A., Nagle, J.M., Perera, R.M., Lapouge, M., Deshpande, V., Zhu, A.X., Lai, A., Min, B., Hoshida, Y., Avruch, J., Sia, D., Campreciós, G., McClatchey, A.I., Llovet, J.M., Morrissey, D., Raj, L., Bardeesy, N., 2015. YAP Inhibition Restores Hepatocyte Differentiation in Advanced HCC, Leading to Tumor Regression. Cell Rep. 10, 1692–1707. doi:10.1016/j.celrep.2015.02.027

Flowers, S., Nagl, N.G., Beck, G.R., Moran, E., 2009. Antagonistic roles for BRM and BRG1 SWI/SNF complexes in differentiation. J. Biol. Chem. 284, 10067–75. doi:10.1074/jbc.M808782200

Friedmann-Morvinski, D., Bushong, E.A., Ke, E., Soda, Y., Marumoto, T., Singer, O., Ellisman, M.H., Verma, I.M., 2012. Dedifferentiation of neurons and astrocytes by oncogenes can induce gliomas in mice. Science 338, 1080–4. doi:10.1126/science.1226929

Gao, X., Tate, P., Hu, P., Tjian, R., Skarnes, W.C., Wang, Z., 2008. ES cell pluripotency and germ-layer formation require the SWI/SNF chromatin remodeling component BAF250a. Proc. Natl. Acad. Sci. U. S. A. 105, 6656–61. doi:10.1073/pnas.0801802105

Gong, F., Fahy, D., Smerdon, M.J., 2006. Rad4-Rad23 interaction with SWI/SNF links ATP-dependent chromatin remodeling with nucleotide excision repair. Nat. Struct. Mol. Biol. 13, 902–7. doi:10.1038/nsmb1152

Gregorieff, A., Liu, Y., Inanlou, M.R., Khomchuk, Y., Wrana, J.L., 2015. Yap-dependent reprogramming of Lgr5+ stem cells drives intestinal regeneration and cancer. Nature. doi:10.1038/nature15382

Guidi, C.J., Sands, A.T., Zambrowicz, B.P., Turner, T.K., Demers, D.A., Webster, W., Smith, T.W., Imbalzano, A.N., Jones, S.N., 2001a. Disruption of Ini1 leads to peri-implantation lethality and tumorigenesis in mice. Mol. Cell. Biol. 21, 3598–603. doi:10.1128/MCB.21.10.3598-3603.2001

Guidi, C.J., Sands, A.T., Zambrowicz, B.P., Turner, T.K., Demers, D.A., Webster, W., Smith, T.W., Imbalzano, A.N., Jones, S.N., 2001b. Disruption of Ini1 leads to peri-implantation lethality and tumorigenesis in mice. Mol. Cell. Biol. 21, 3598–603. doi:10.1128/MCB.21.10.3598-3603.2001

Gumbiner, B.M., Kim, N.-G., 2014. The Hippo-YAP signaling pathway and contact inhibition of growth. J. Cell Sci. 127, 709–17. doi:10.1242/jcs.140103

Halder, G., Dupont, S., Piccolo, S., 2012. Transduction of mechanical and cytoskeletal cues by YAP and TAZ. Nat. Rev. Mol. Cell Biol. 13, 591–600. doi:10.1038/nrm3416

Hanahan, D., Weinberg, R.A., 2011. Hallmarks of cancer: the next generation. Cell 144, 646–74. doi:10.1016/j.cell.2011.02.013

Hara, R., Sancar, A., 2002. The SWI/SNF chromatin-remodeling factor stimulates repair by human excision nuclease in the mononucleosome core particle. Mol. Cell. Biol. 22, 6779–87.

Hashimoto, T., Suzuki, Y., Tanihara, M., Kakimaru, Y., Suzuki, K., 2004. Development of alginate wound dressings linked with hybrid peptides derived from laminin and elastin. Biomaterials 25, 1407–1414. doi:10.1016/j.biomaterials.2003.07.004

Helming, K.C., Wang, X., Roberts, C.W.M., 2014. Vulnerabilities of Mutant SWI/SNF Complexes in Cancer. Cancer Cell 26, 309–317. doi:10.1016/j.ccr.2014.07.018

Ho, L., Ronan, J.L., Wu, J., Staahl, B.T., Chen, L., Kuo, A., Lessard, J., Nesvizhskii, A.I., Ranish, J., Crabtree, G.R., 2009. An embryonic stem cell chromatin remodeling complex, esBAF, is essential for embryonic stem cell self-renewal and pluripotency. Proc. Natl. Acad. Sci. U. S. A. 106, 5181–6. doi:10.1073/pnas.0812889106

Hu, G., Schones, D.E., Cui, K., Ybarra, R., Northrup, D., Tang, Q., Gattinoni, L., Restifo, N.P., Huang, S., Zhao, K., 2011. Regulation of nucleosome landscape and transcription factor targeting at tissue-specific enhancers by BRG1. Genome Res. 21, 1650–8. doi:10.1101/gr.121145.111

Huang, J., Wu, S., Barrera, J., Matthews, K., Pan, D., 2005. The Hippo signaling pathway coordinately regulates cell proliferation and apoptosis by inactivating Yorkie, the Drosophila Homolog of YAP. Cell 122, 421–34. doi:10.1016/j.cell.2005.06.007

Ito, M., Liu, Y., Yang, Z., Nguyen, J., Liang, F., Morris, R.J., Cotsarelis, G., 2005. Stem cells in the hair follicle bulge contribute to wound repair but not to homeostasis of the epidermis. Nat. Med. 11, 1351–4. doi:10.1038/nm1328

Jones, S., Wang, T.-L., Shih, I.-M., Mao, T.-L., Nakayama, K., Roden, R., Glas, R., Slamon, D., Diaz, L.A., Vogelstein, B., Kinzler, K.W., Velculescu, V.E., Papadopoulos, N., 2010. Frequent mutations of chromatin remodeling gene ARID1A in ovarian clear cell carcinoma. Science 330, 228–31. doi:10.1126/science.1196333

Kadam, S., 2000. Functional selectivity of recombinant mammalian SWI/SNF subunits. Genes Dev. 14, 2441–2451. doi:10.1101/gad.828000

Kadoch, C., Crabtree, G.R., 2015. Mammalian SWI / SNF chromatin remodeling complexes and cancer : Mechanistic insights gained from human genomics 1–17.

Kanellos, G., Zhou, J., Patel, H., Ridgway, R.A., Huels, D., Gurniak, C.B., Sandilands, E., Carragher, N.O., Sansom, O.J., Witke, W., Brunton, V.G., Frame, M.C., 2015. ADF and Cofilin1 Control Actin Stress Fibers, Nuclear Integrity, and Cell Survival. Cell Rep. 13, 1949–1964. doi:10.1016/j.celrep.2015.10.056

Kassabov, S.R., Zhang, B., Persinger, J., Bartholomew, B., 2003. SWI/SNF Unwraps, Slides, and Rewraps the Nucleosome. Mol. Cell 11, 391–403. doi:10.1016/S1097-2765(03)00039-X

Kidder, B.L., Palmer, S., Knott, J.G., 2009. SWI/SNF-Brg1 regulates self-renewal and occupies core pluripotency-related genes in embryonic stem cells. Stem Cells 27, 317–28. doi:10.1634/stemcells.2008-0710

Klochendler-Yeivin, A., Fiette, L., Barra, J., Muchardt, C., Babinet, C., Yaniv, M., 2000. The murine SNF5/INI1 chromatin remodeling factor is essential for embryonic development and tumor suppression. EMBO Rep. 1, 500–6. doi:10.1093/embo-reports/kvd129

Koe, C.T., Li, S., Rossi, F., Jing, J., Wong, L., Wang, Y., Zhang, Z., Chen, K., Aw, S.S., Richardson, H.E., 2014. The Brm-HDAC3-Erm repressor complex suppresses dedifferentiation in Drosophila type II neuroblast lineages. E-life 1–19. doi:10.7554/eLife.01906

Lau, A.N., Curtis, S.J., Fillmore, C.M., Rowbotham, S.P., Mohseni, M., Wagner, D.E., Beede, A.M., Montoro, D.T., Sinkevicius, K.W., Walton, Z.E., Barrios, J., Weiss, D.J., Camargo, F.D., Wong, K.-K., Kim, C.F., 2014. Tumor-propagating cells and Yap/Taz activity contribute to lung tumor progression and metastasis. EMBO J. 33, 468–81. doi:10.1002/embj.201386082

Lessard, J., Wu, J.I., Ranish, J. a, Wan, M., Winslow, M.M., Staahl, B.T., Wu, H., Aebersold, R., Graef, I. a, Crabtree, G.R., 2007. An essential switch in subunit composition of a chromatin remodeling complex during neural development. Neuron 55, 201–15. doi:10.1016/j.neuron.2007.06.019

Lickert, H., Takeuchi, J.K., Von Both, I., Walls, J.R., McAuliffe, F., Adamson, S.L., Henkelman, R.M., Wrana, J.L., Rossant, J., Bruneau, B.G., 2004. Baf60c is essential for function of BAF chromatin remodelling complexes in heart development. Nature 432, 107–12. doi:10.1038/nature03071

Lin, Z., Pu, W.T., 2014. Harnessing Hippo in the heart: Hippo/Yap signaling and applications to heart regeneration and rejuvenation. Stem Cell Res. 13, 571–81. doi:10.1016/j.scr.2014.04.010

Lu, L., Li, Y., Kim, S.M., Bossuyt, W., Liu, P., Qiu, Q., Wang, Y., Halder, G., Finegold, M.J., Lee, J.-S., Johnson, R.L., 2010. Hippo signaling is a potent in vivo growth and tumor suppressor pathway in the mammalian liver. Proc. Natl. Acad. Sci. U. S. A. 107, 1437–42. doi:10.1073/pnas.0911427107

Mammoto, A., Ingber, D.E., 2009. Cytoskeletal control of growth and cell fate switching. Curr. Opin. Cell Biol. 21, 864–70. doi:10.1016/j.ceb.2009.08.001

Mast, B.A., Schultz, G.S., 1996. Interactions of cytokines, growth factors, and proteases in acute and chronic wounds. Wound Repair Regen. 4, 411–20.

doi:10.1046/j.1524-475X.1996.40404.x
Navarro-Lérida, I., Pellinen, T., Sanchez, S.A., Guadamillas, M.C., Wang, Y., Mirtti, T., Calvo, E., Del Pozo, M.A., 2015. Rac1 Nucleocytoplasmic Shuttling Drives Nuclear Shape Changes and Tumor Invasion. Dev. Cell 32, 318–334. doi:10.1016/j.devcel.2014.12.019
Nejak-Bowen, K., Okabe, H., Monga, S., 2015. Wnt/Beta-Catenin Cooperates With Yap Signaling To Promote Hepatobiliary Repair In A Model Of Chronic Liver Injury. FASEB J 29, 416.7–.
Nishimoto, N., Watanabe, M., Watanabe, S., Sugimoto, N., Yugawa, T., Ikura, T., Koiwai, O., Kiyono, T., Fujita, M., 2012. Heterocomplex formation by Arp4 and β-actin is involved in the integrity of the Brg1 chromatin remodeling complex. J. Cell Sci. 125, 3870–82. doi:10.1242/jcs.104349
Oren, M., 2013. The Hippo Signaling Pathway and Cancer. Springer New York, New York, NY. doi:10.1007/978-1-4614-6220-0
Park, J.-H., Park, E.-J., Lee, H.-S., Kim, S.J., Hur, S.-K., Imbalzano, A.N., Kwon, J., 2006. Mammalian SWI/SNF complexes facilitate DNA double-strand break repair by promoting gamma-H2AX induction. EMBO J. 25, 3986–97. doi:10.1038/sj.emboj.7601291
Parsons, J.T., Horwitz, A.R., Schwartz, M.A., 2010. Cell adhesion: integrating cytoskeletal dynamics and cellular tension. Nat. Rev. Mol. Cell Biol. 11, 633–43. doi:10.1038/nrm2957
Phelan, M.L., Sif, S., Narlikar, G.J., Kingston, R.E., 1999. Reconstitution of a Core Chromatin Remodeling Complex from SWI/SNF Subunits. Mol. Cell 3, 247–253. doi:10.1016/S1097-2765(00)80315-9
Piccolo, S., Cordenonsi, M., Dupont, S., 2013. Molecular pathways: YAP and TAZ take center stage in organ growth and tumorigenesis. Clin. Cancer Res. 19, 4925–30. doi:10.1158/1078-0432.CCR-12-3172
Piccolo, S., Dupont, S., Cordenonsi, M., 2014. The biology of YAP/TAZ: hippo signaling and beyond. Physiol. Rev. 94, 1287–312. doi:10.1152/physrev.00005.2014
Plessner, M., Melak, M., Chinchilla, P., Baarlink, C., Grosse, R., 2015. Nuclear F-actin formation and reorganization upon cell spreading. J. Biol. Chem. 290, 11208–11216. doi:10.1074/jbc.M114.627166
Ramos, A., Camargo, F.D., 2012. The Hippo signaling pathway and stem cell biology. Trends Cell Biol. 22, 339–46. doi:10.1016/j.tcb.2012.04.006
Rando, O.J., Zhao, K., Janmey, P., Crabtree, G.R., 2002. Phosphatidylinositol-dependent actin filament binding by the SWI/SNF-like BAF chromatin remodeling complex. Proc. Natl. Acad. Sci. U. S. A. 99, 2824–9. doi:10.1073/pnas.032662899
Roberts, C.W., Galusha, S.A., McMenamin, M.E., Fletcher, C.D., Orkin, S.H., 2000. Haploinsufficiency of Snf5 (integrase interactor 1) predisposes to malignant rhabdoid tumors in mice. Proc. Natl. Acad. Sci. U. S. A. 97, 13796–800. doi:10.1073/pnas.250492697
Roberts, C.W.M., Leroux, M.M., Fleming, M.D., Orkin, S.H., 2002. Highly

penetrant, rapid tumorigenesis through conditional inversion of the tumor suppressor gene Snf5. Cancer Cell 2, 415–25.

Sansores-Garcia, L., Bossuyt, W., Wada, K.-I., Yonemura, S., Tao, C., Sasaki, H., Halder, G., 2011. Modulating F-actin organization induces organ growth by affecting the Hippo pathway. EMBO J. 30, 2325–35. doi:10.1038/emboj.2011.157

Santner, S.J., Dawson, P.J., Tait, L., Soule, H.D., Eliason, J., Mohamed, A.N., Wolman, S.R., Heppner, G.H., Miller, F.R., 2001. Malignant MCF10CA1 cell lines derived from premalignant human breast epithelial MCF10AT cells. Breast Cancer Res. Treat. 65, 101–10.

Schwitalla, S., Fingerle, A.A., Cammareri, P., Nebelsiek, T., Göktuna, S.I., Ziegler, P.K., Canli, O., Heijmans, J., Huels, D.J., Moreaux, G., Rupec, R.A., Gerhard, M., Schmid, R., Barker, N., Clevers, H., Lang, R., Neumann, J., Kirchner, T., Taketo, M.M., van den Brink, G.R., Sansom, O.J., Arkan, M.C., Greten, F.R., 2013. Intestinal tumorigenesis initiated by dedifferentiation and acquisition of stem-cell-like properties. Cell 152, 25–38. doi:10.1016/j.cell.2012.12.012

Singhal, N., Graumann, J., Wu, G., Araúzo-Bravo, M.J., Han, D.W., Greber, B., Gentile, L., Mann, M., Schöler, H.R., 2010. Chromatin-Remodeling Components of the BAF Complex Facilitate Reprogramming. Cell 141, 943–55. doi:10.1016/j.cell.2010.04.037

Skibinski, A., Breindel, J.L., Prat, A., Galván, P., Smith, E., Rolfs, A., Gupta, P.B., Labaer, J., Kuperwasser, C., 2014. The Hippo transducer TAZ interacts with the SWI/SNF complex to regulate breast epithelial lineage commitment. Cell Rep. 6, 1059–72. doi:10.1016/j.celrep.2014.02.038

Stewart, S. a, Dykxhoorn, D.M., Palliser, D., Mizuno, H., Yu, E.Y., An, D.S., Sabatini, D.M., Chen, I.S.Y., Hahn, W.C., Sharp, P. a, Weinberg, R. a, Novina, C.D., 2003. Lentivirus-delivered stable gene silencing by RNAi in primary cells Lentivirus-delivered stable gene silencing by RNAi in primary cells. Rna 9, 493–501. doi:10.1261/rna.2192803.rapid

Stüven, T., Hartmann, E., Görlich, D., 2003. Exportin 6: a novel nuclear export receptor that is specific for profilin.actin complexes. EMBO J. 22, 5928–40. doi:10.1093/emboj/cdg565

Szerlong, H., Hinata, K., Viswanathan, R., Erdjument-Bromage, H., Tempst, P., Cairns, B.R., 2008. The HSA domain binds nuclear actin-related proteins to regulate chromatin-remodeling ATPases. Nat. Struct. Mol. Biol. 15, 469–76. doi:10.1038/nsmb.1403

Tolstorukov, M.Y., Sansam, C.G., Lu, P., Koellhoffer, E.C., Helming, K.C., Alver, B.H., Tillman, E.J., Evans, J.A., Wilson, B.G., Park, P.J., Roberts, C.W.M., 2013. Swi/Snf chromatin remodeling/tumor suppressor complex establishes nucleosome occupancy at target promoters. Proc. Natl. Acad. Sci. U. S. A. 110, 10165–70. doi:10.1073/pnas.1302209110

Tsuruta, D., Hashimoto, T., Hamill, K.J., Jones, J.C.R., 2011. Hemidesmosomes and focal contact proteins: functions and cross-talk in keratinocytes, bullous

diseases and wound healing. J. Dermatol. Sci. 62, 1–7. doi:10.1016/j.jdermsci.2011.01.005

Wada, K.-I., Itoga, K., Okano, T., Yonemura, S., Sasaki, H., 2011. Hippo pathway regulation by cell morphology and stress fibers. Development 138, 3907–3914. doi:10.1242/dev.070987

Wang, W., Côté, J., Xue, Y., Zhou, S., Khavari, P.A., Biggar, S.R., Muchardt, C., Kalpana, G. V, Goff, S.P., Yaniv, M., Workman, J.L., Crabtree, G.R., 1996. Purification and biochemical heterogeneity of the mammalian SWI-SNF complex. EMBO J. 15, 5370–82.

Watanabe, R., Ui, A., Kanno, S.-I., Ogiwara, H., Nagase, T., Kohno, T., Yasui, A., 2014. SWI/SNF factors required for cellular resistance to DNA damage include ARID1A and ARID1B and show interdependent protein stability. Cancer Res. 74, 2465–75. doi:10.1158/0008-5472.CAN-13-3608

Wilson, B.G., Roberts, C.W.M., 2011. SWI/SNF nucleosome remodellers and cancer. Nat. Rev. Cancer 11, 481–92. doi:10.1038/nrc3068

Wilson, B.G., Wang, X., Shen, X., McKenna, E.S., Lemieux, M.E., Cho, Y.-J., Koellhoffer, E.C., Pomeroy, S.L., Orkin, S.H., Roberts, C.W.M., 2010. Epigenetic antagonism between polycomb and SWI/SNF complexes during oncogenic transformation. Cancer Cell 18, 316–28. doi:10.1016/j.ccr.2010.09.006

Wozniak, M.A., Chen, C.S., 2009. Mechanotransduction in development: a growing role for contractility. Nat. Rev. Mol. Cell Biol. 10, 34–43. doi:10.1038/nrm2592

Wu, J.I., Lessard, J., Crabtree, G.R., 2009. Understanding the words of chromatin regulation. Cell 136, 200–6. doi:10.1016/j.cell.2009.01.009

Wu, J.I., Lessard, J., Olave, I. a, Qiu, Z., Ghosh, A., Graef, I. a, Crabtree, G.R., 2007. Regulation of dendritic development by neuron-specific chromatin remodeling complexes. Neuron 56, 94–108. doi:10.1016/j.neuron.2007.08.021

Xin, M., Kim, Y., Sutherland, L.B., Qi, X., McAnally, J., Schwartz, R.J., Richardson, J.A., Bassel-Duby, R., Olson, E.N., 2011. Regulation of insulin-like growth factor signaling by Yap governs cardiomyocyte proliferation and embryonic heart size. Sci. Signal. 4, ra70. doi:10.1126/scisignal.2002278

Yan, Z., Wang, Z., Sharova, L., Sharov, A. a, Ling, C., Piao, Y., Aiba, K., Matoba, R., Wang, W., Ko, M.S.H., 2008. BAF250B-associated SWI/SNF chromatin-remodeling complex is required to maintain undifferentiated mouse embryonic stem cells. Stem Cells 26, 1155–65. doi:10.1634/stemcells.2007-0846

Yimlamai, D., Christodoulou, C., Galli, G.G., Yanger, K., Pepe-Mooney, B., Gurung, B., Shrestha, K., Cahan, P., Stanger, B.Z., Camargo, F.D., 2014a. Hippo Pathway Activity Influences Liver Cell Fate. Cell 157, 1324–1338. doi:10.1016/j.cell.2014.03.060

Yimlamai, D., Christodoulou, C., Galli, G.G., Yanger, K., Pepe-Mooney, B.,

Gurung, B., Shrestha, K., Cahan, P., Stanger, B.Z., Camargo, F.D., 2014b. Hippo pathway activity influences liver cell fate. Cell 157, 1324–38. doi:10.1016/j.cell.2014.03.060

Yin, F., Yu, J., Zheng, Y., Chen, Q., Zhang, N., Pan, D., 2013a. Spatial organization of Hippo signaling at the plasma membrane mediated by the tumor suppressor Merlin/NF2. Cell 154, 1342–55. doi:10.1016/j.cell.2013.08.025

Yin, F., Yu, J., Zheng, Y., Chen, Q., Zhang, N., Pan, D., 2013b. Spatial organization of Hippo signaling at the plasma membrane mediated by the tumor suppressor Merlin/NF2. Cell 154, 1342–55. doi:10.1016/j.cell.2013.08.025

Young, D.W., Pratap, J., Javed, A., Weiner, B., Ohkawa, Y., van Wijnen, A., Montecino, M., Stein, G.S., Stein, J.L., Imbalzano, A.N., Lian, J.B., 2005. SWI/SNF chromatin remodeling complex is obligatory for BMP2-induced, Runx2-dependent skeletal gene expression that controls osteoblast differentiation. J. Cell. Biochem. 94, 720–30. doi:10.1002/jcb.20332

Yu, Y., Chen, Y., Kim, B., Wang, H., Zhao, C., He, X., Liu, L., Liu, W., Wu, L.M.N., Mao, M., Chan, J.R., Wu, J., Lu, Q.R., 2013. Olig2 targets chromatin remodelers to enhancers to initiate oligodendrocyte differentiation. Cell 152, 248–61. doi:10.1016/j.cell.2012.12.006

Zanconato, F., Forcato, M., Battilana, G., Azzolin, L., Quaranta, E., Bodega, B., Rosato, A., Bicciato, S., Cordenonsi, M., Piccolo, S., 2015. Genome-wide association between YAP/TAZ/TEAD and AP-1 at enhancers drives oncogenic growth. Nat. Cell Biol. doi:10.1038/ncb3216

Zanconato, F., Piccolo, S., 2015. Eradicating tumor drug resistance at its YAP-biomechanical roots. EMBO J. e201593584. doi:10.15252/embj.201593584

Zhang, H., Liu, C.-Y., Zha, Z.-Y., Zhao, B., Yao, J., Zhao, S., Xiong, Y., Lei, Q.-Y., Guan, K.-L., 2009. TEAD transcription factors mediate the function of TAZ in cell growth and epithelial-mesenchymal transition. J. Biol. Chem. 284, 13355–62. doi:10.1074/jbc.M900843200

Zhao, B., Tumaneng, K., Guan, K.-L., 2011a. The Hippo pathway in organ size control, tissue regeneration and stem cell self-renewal. Nat. Cell Biol. 13, 877–83. doi:10.1038/ncb2303

Zhao, B., Tumaneng, K., Guan, K.-L., 2011b. The Hippo pathway in organ size control, tissue regeneration and stem cell self-renewal. Nat. Cell Biol. 13, 877–83. doi:10.1038/ncb2303

Zhao, B., Ye, X., Yu, J., Li, L., Li, W., Li, S., Yu, J., Lin, J.D., Wang, C., Chinnaiyan, A.M., Lai, Z., Guan, K., 2008. TEAD mediates YAP-dependent gene induction and growth control 1962–1971. doi:10.1101/gad.1664408.2007

Zhao, K., Wang, W., Rando, O.J., Xue, Y., Swiderek, K., Kuo, a, Crabtree, G.R., 1998. Rapid and phosphoinositol-dependent binding of the SWI/SNF-like BAF complex to chromatin after T lymphocyte receptor signaling. Cell 95,

625–36.
Zhao, R., Fallon, T.R., Saladi, S.V., Pardo-Saganta, A., Villoria, J., Mou, H., Vinarsky, V., Gonzalez-Celeiro, M., Nunna, N., Hariri, L.P., Camargo, F., Ellisen, L.W., Rajagopal, J., 2014. Yap Tunes Airway Epithelial Size and Architecture by Regulating the Identity, Maintenance, and Self-Renewal of Stem Cells. Dev. Cell 1–15. doi:10.1016/j.devcel.2014.06.004
Zraly, C.B., Middleton, F.A., Dingwall, A.K., 2006. Hormone-response Genes Are Direct in Vivo Regulatory Targets of Brahma (SWI/SNF) Complex Function. J. Biol. Chem. 281, 35305–35315. doi:10.1074/jbc.M607806200

TABLES

Table 1. PCR oligo sequences. Related to Experimental Procedures.

Gene	Forward primer	Reverse primer
human		
GAPDH	AGCCACATCGCTCAGACAC	GCCCAATACGACCAAATCC
ANKRD1	AGTAGAGGAACTGGTCACTGG	TGGGCTAGAAGTGTCTTCAGAT
PTX3	TGCATCTCCTTGCGATTCTG	GAGCTTGTCCCATTCCGAGT
CYR61:	CCTTGTGGACAGCCAGTGTA	ACTTGGGCCGGTATTTCTTC
CTGF	AGGAGTGGGTGTGTGACGA	CCAGGCAGTTGGCTCTAATC
ARID1a	GGGGCGCCTCCTCACT	CTTTGTTGTCCGCCATGTTG
BRG1	CGCATTCGCAACCACAAGTA	CCTCACTCTCCTCGCCTTCA
BRM	CCCCCAAACTGACAAAGCAG	CTGAGCTGTCGCCCTGAACT
mouse		
Gapdh	ATCCTGCACCACCAACTGCT	GGGCCATCCACAGTCTTCTG
Arid1a	TGAAAGACATTGGAACCCCG	TCTAGCAAGCCTGGGAGCTG
Brm	ATCTTCAGGCGGCAGACACG	ATCTTCAGGCGGCAGACACG

Table 2. RNAi sequences. Related to Experimental Procedures.

siRNA/ shRNA	**Interfering sequence** (target)
Control#1	AllStars Negative Control siRNA (QIAGEN)
Control#2	TTCTCCGAACGTGTCACGT
human	
ARID1a#1	GGCGGGAACTTGCAACCAA
ARID1a#2	CGGTATCACCGTTGATGAA
BRG1#1	GCGCTACAACCAGATGAAA
BRG1#2	ACTGGATGTCAAACAGTAA
BRM#1	GCGTCTACATAAGGTGTTA
BRM#2	CCGCATAGCTCATAGGATA
YAP#1	GACATCTTCTGGTCAGAGA
YAP#2	CTGGTCAGAGATACTTCTT
TAZ#1	ACGTTGACTTAGGAACTTT
TAZ#2	AGGTACTTCCTCAATCACA
LATS1	CACGGCAAGATAGCATGGA
LATS2	AAAGGCGTATGGCGAGTAG
mouse	
Arid1a#5	CACCATTAACATTCTACTGTA
Arid1a#6	CACGTGTTAAGAATAAATGTA
Brm#1	CAGGAAAGACTTACCAGAATA
Brm#2	TACCAGAATACTATGAATTAA

Table 3. Some positive results of MS

		untreated	untreated	Lat.A	Lat.A
Accession Number	**MW**	**-**	**Flag-YAP-5SA**	**Flag-YAP -5SA**	**-**
TEAD1_HUMAN	48 kDa	0	6	4	0
TEAD2_HUMAN	49 kDa	0	1	1	0
TEAD3_HUMAN	49 kDa	0	16	9	0
TEAD4_HUMAN	48 kDa	0	4	1	0
LATS1_HUMAN	127 kDa	0	17	29	0
LATS2_HUMAN	120 kDa	0	6	15	0
ZYX_HUMAN	61 kDa	0	2	2	0
MPDZ_HUMAN	222 kDa	0	19	52	0
PTN14_HUMAN	135 kDa	0	29	62	0
WWC2_HUMAN	134 kDa	0	1	4	0
WWC3_HUMAN	123 kDa	0	9	13	0
CTNA1_HUMAN	100 kDa	1	1	0	3
ZO1_HUMAN	195 kDa	0	0	3	0
ZO2_HUMAN	134 kDa	0	1	5	0
INADL_HUMAN	196 kDa	0	23	41	0
LIN7C_HUMAN	22 kDa	0	4	5	0
MERL_HUMAN	70 kDa	0	21	27	0
MPP5_HUMAN	77 kDa	0	9	27	0
AMOL1_HUMAN	107 kDa	0	30	30	0
AMOL2_HUMAN	86 kDa	0	44	68	0

Table 4. Results of MS

		untreated	untreated	Lat.A	Lat.A
Accession Number	MW	-	Flag-YAP-5SA	Flag-YAP -5SA	-
ARID1A_HUMAN	242 kDa	0	4	11	0
ARID1B_HUMAN	236 kDa	0	0	4	0
BRG1_HUMAN	185 kDa	0	2	10	0
SMARCC1_HUMAN	123 kDa	0	1	8	0
BAF53a_HUMAN	47 kDa	0	3	1	0
SMARCA5_HUMAN	122 kDa	0	1	2	0
PARD3_HUMAN	151 kDa	0	0	8	0
RPGF6_HUMAN	179 kDa	0	0	7	0
EZRI_HUMAN	69 kDa	0	0	4	0
UBA1_HUMAN	118 kDa	0	0	4	0
CTRO_HUMAN	231 kDa	0	0	3	0
CKAP4_HUMAN	66 kDa	0	0	3	0
RASF8_HUMAN	48 kDa	0	0	2	0
ARHG2_HUMAN	112 kDa	0	0	2	0
CAP1_HUMAN	52 kDa	0	1	2	1
TPPC9_HUMAN	129 kDa	0	0	2	0
IF4G1_HUMAN	175 kDa	0	0	2	0
C1TM_HUMAN	106 kDa	0	0	2	0
TET2_HUMAN	224 kDa	0	0	2	0
E2F7_HUMAN	100 kDa	0	0	2	0
EMD_HUMAN	29 kDa	0	0	2	0
HMHA1_HUMAN	125 kDa	0	0	2	0
HNRL1_HUMAN	96 kDa	0	0	2	0
MCM2_HUMAN	102 kDa	0	0	2	0
MSH6_HUMAN	153 kDa	0	0	2	0
RNC_HUMAN	159 kDa	0	0	2	0
STAT1_HUMAN	87 kDa	0	0	2	0
XRCC5_HUMAN	83 kDa	0	29	38	0
XRCC6_HUMAN	70 kDa	0	34	36	2
MYH9_HUMAN	227 kDa	3	22	33	2
ANM5_HUMAN	73 kDa	3	12	15	1

FIGURES

Figure 1. Introduction

A. Schematic representation of the Hippo pathway.

B. Schematic representation of how mechanic cues regulate YAP/TAZ

C. Schematic representation of YAP induced reprogramming.

D. Schematic representation of SWI/SNF complexes.

Figure 1

A

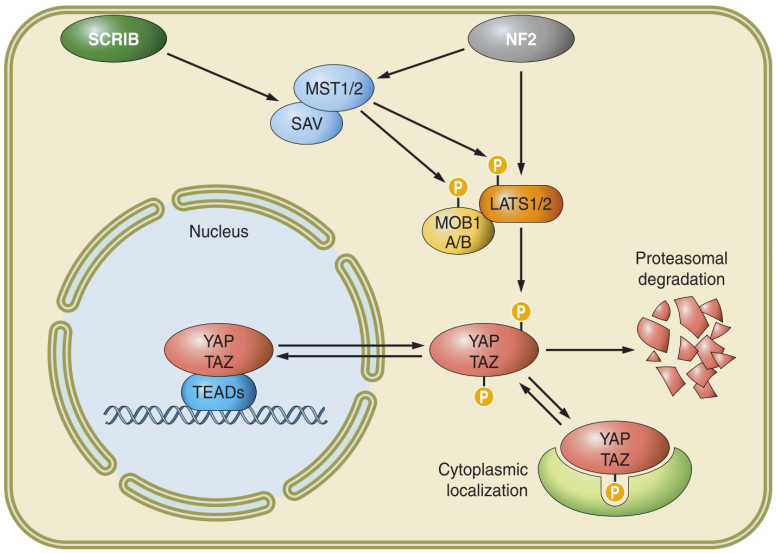

B

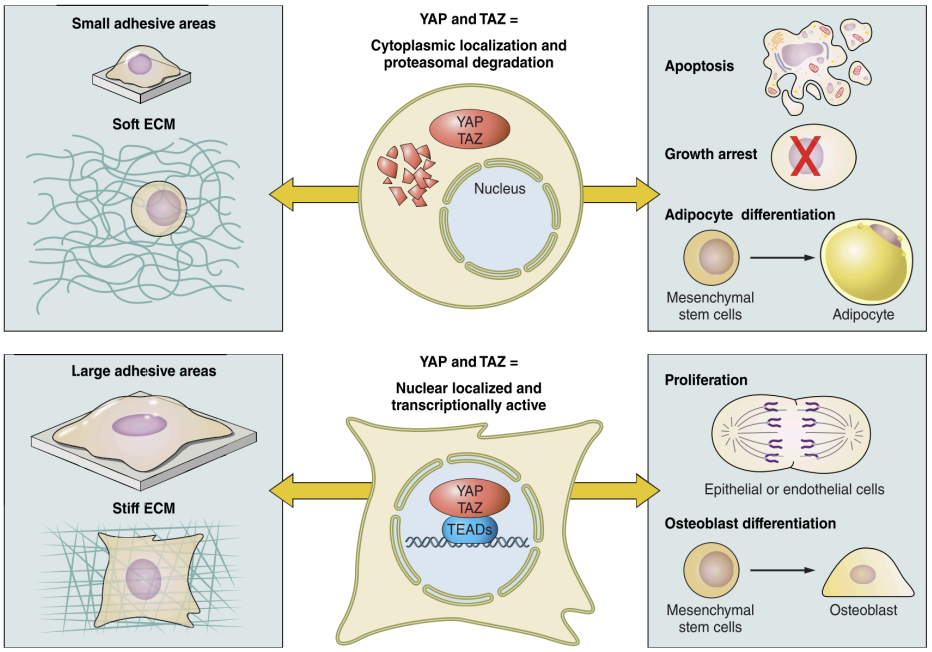

C

D

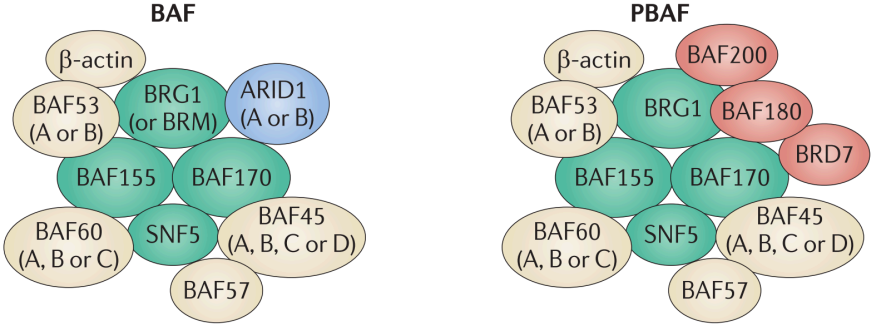

Figure 2. Treatment with Latrunculin A in sparse epithelial mammary cells causes YAP/TAZ transcriptional inhibition that can not be rescued by blocking YAP/TAZ nuclear export

A. Schematic representation of the experimental procedure. MCF10A cells were plated at low confluence (sparse) and, after attachment, treated with Latrunculin (Lat.A; 0.5 μM) and Leptomycin B (LMB; 15 ng/mL) as indicated, and then fixed for immunofluorescence or harvested for RNA extraction.

B. MCF10A cells were treated as in A and stained for immunofluorescence with anti-YAP/TAZ antibody. Phalloidin shows cell border and the effect of Lat.A. Nuclei were couterstained with DAPI.

C. Quantifications of **Figure 2B**. The panel shows the proportion of cells displaying: N+N/C, nuclear YAP/TAZ localization or even distribution in the nucleus and cytosol; or C, cytosol YAP/TAZ localization.

D. MCF10A cells were treated as in A and harvested for RNA extraction. Panels are qRT-PCR results for *CYR61* and *ANKRD1,* expression normalized to *GAPDH* expression. Data are normalized to untreated cells and presented as mean + SD.

Figure 2

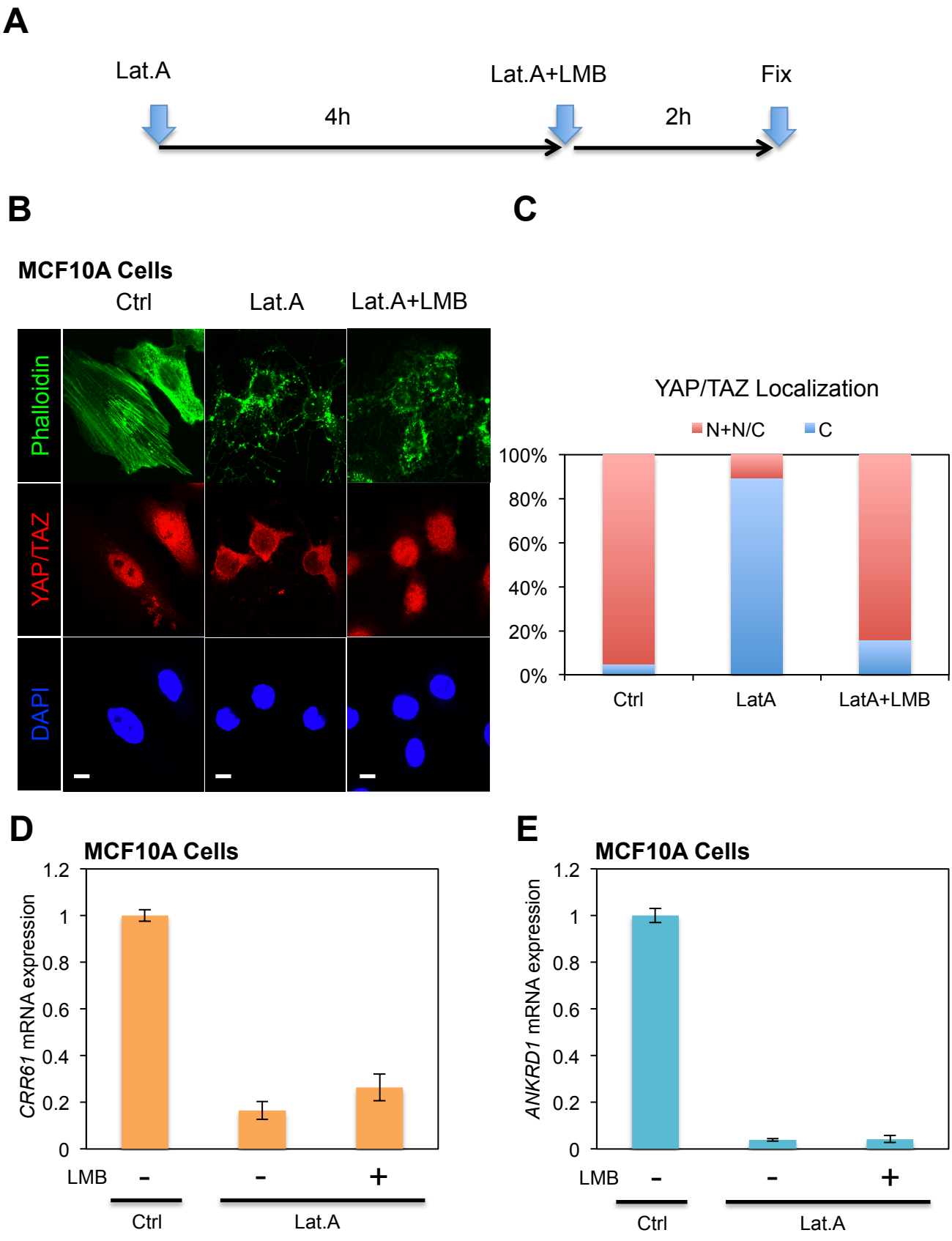
A
Lat.A
4h
Lat.A+LMB
2h
Fix
B
MCF10A Cells
Ctrl
Lat.A
Lat.A+LMB
Phalloidin
YAP/TAZ
DAPI
C
YAP/TAZ Localization
N+N/C
C
100%
80%
60%
40%
20%
0%
Ctrl
LatA
LatA+LMB
D
MCF10A Cells
CRR61 mRNA expression
1.2
1
0.8
0.6
0.4
0.2
0
LMB
-
-
+
Ctrl
Lat.A
E
MCF10A Cells
ANKRD1 mRNA expression
1.2
1
0.8
0.6
0.4
0.2
0
LMB
-
-
+
Ctrl
Lat.A

Figure 3. High cell densitiy leads to YAP/TAZ transcriptional inhibition that can not be rescued by blocking YAP/TAZ nuclear export

A. Schematic representation of the experimental procedure. MCF10A cells were plated at high confluence (dense) and, after 24 hours, treated with LMB, as indicated, and then fixed for immunofluorescence or harvested for RNA extraction.

B. MCF10A cells were treated as in A and stained for immunofluorescence with anti-YAP/TAZ antibody. Nuclei were couterstained with DAPI.

C. Quantifications of **Figure 3B**. The panel shows the proportion of cells displaying: N+N/C, nuclear YAP/TAZ localization or even distribution in the nucleus and cytosol; or C, cytosol YAP/TAZ localization.

D. MCF10A cells were treated as in A and harvested for RNA extraction. Panels are qRT-PCR results for *CYR61* and *PTX3* expression, normalized to *GAPDH* expression. Data are normalized to sparse cells and presented as mean + SD.

Figure 3

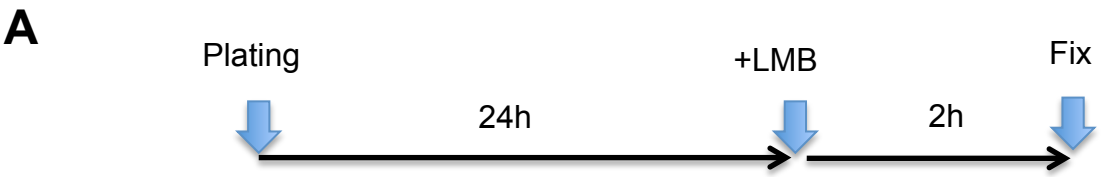
A
Plating
24h
+LMB
2h
Fix

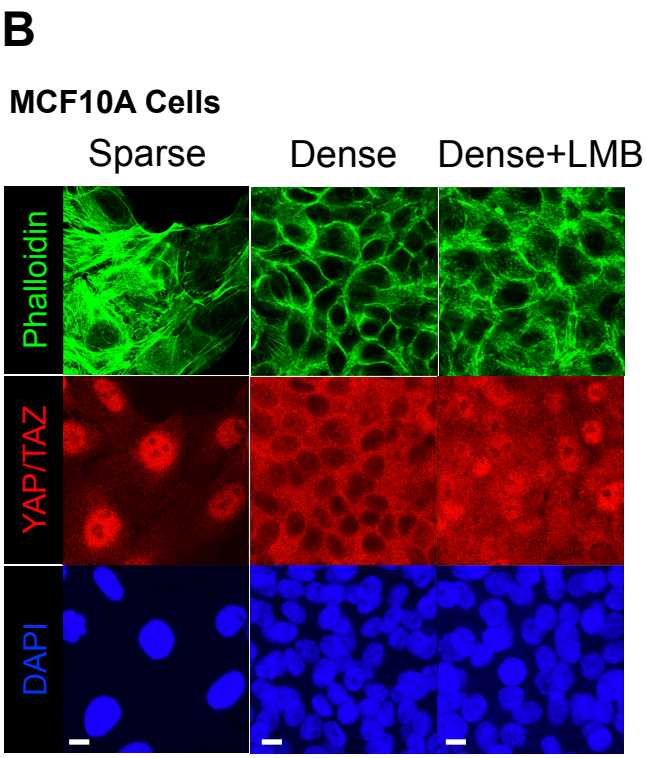
B
MCF10A Cells
Sparse
Dense
Dense+LMB
Phalloidin
YAP/TAZ
DAPI

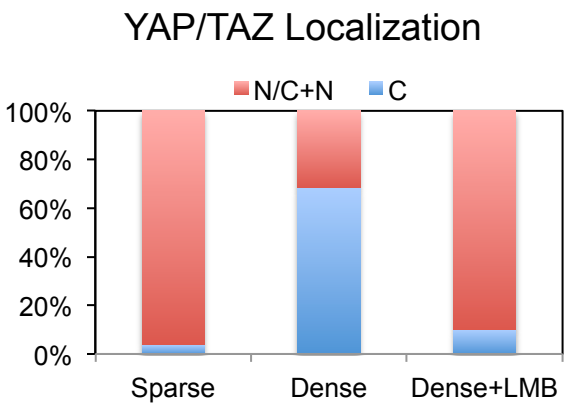
C
YAP/TAZ Localization
N/C+N
C
100%
80%
60%
40%
20%
0%
Sparse
Dense
Dense+LMB

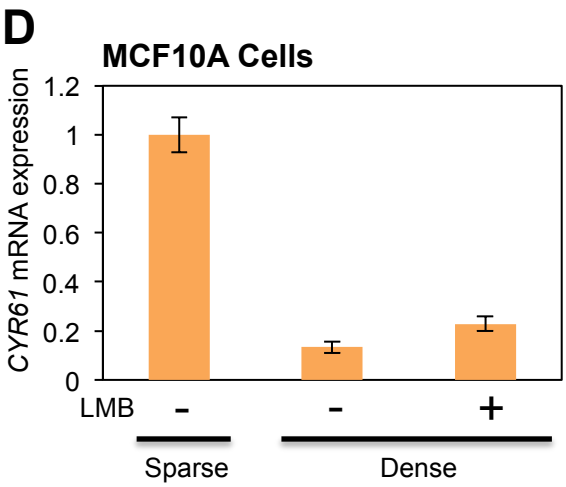
D
MCF10A Cells
CYR61 mRNA expression
1.2
1
0.8
0.6
0.4
0.2
0
LMB
-
-
+
Sparse
Dense

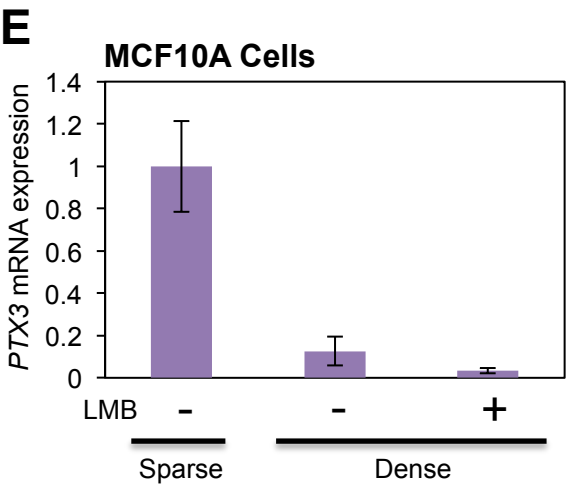
E
MCF10A Cells
PTX3 mRNA expression
1.4
1.2
1
0.8
0.6
0.4
0.2
0
LMB
-
-
+
Sparse
Dense

Figure 4. A soft ECM leads to YAP/TAZ transcriptional inhibition that can not be rescued by blocking YAP/TAZ nuclear export

A. Schematic representation of the experimental procedure. MCF10A cells were plated either on plastic (stiff) or on a soft ECM (hydrogel 0.7 kPa). After 24 hours, cells were treated with LMB, as indicated, and then fixed for immunofluorescence or harvested for RNA extraction.

B. MCF10A cells were treated as in A and stained for immunofluorescence with anti-YAP/TAZ antibody. Nuclei were couterstained with DAPI.

C. Quantifications of **Figure 4B**. The panel shows the proportion of cells displaying: N+N/C, nuclear YAP/TAZ localization or even distribution in the nucleus and cytosol; or C, cytosol YAP/TAZ localization.

D. MCF10A cells were treated as in A and harvested for RNA extraction. Panels are qRT-PCR results for *CYR61* and *PTX3* expression, normalized to *GAPDH* expression. Data are normalized to cells plated on a stiff ECM (plastic) and presented as mean + SD.

Figure 4

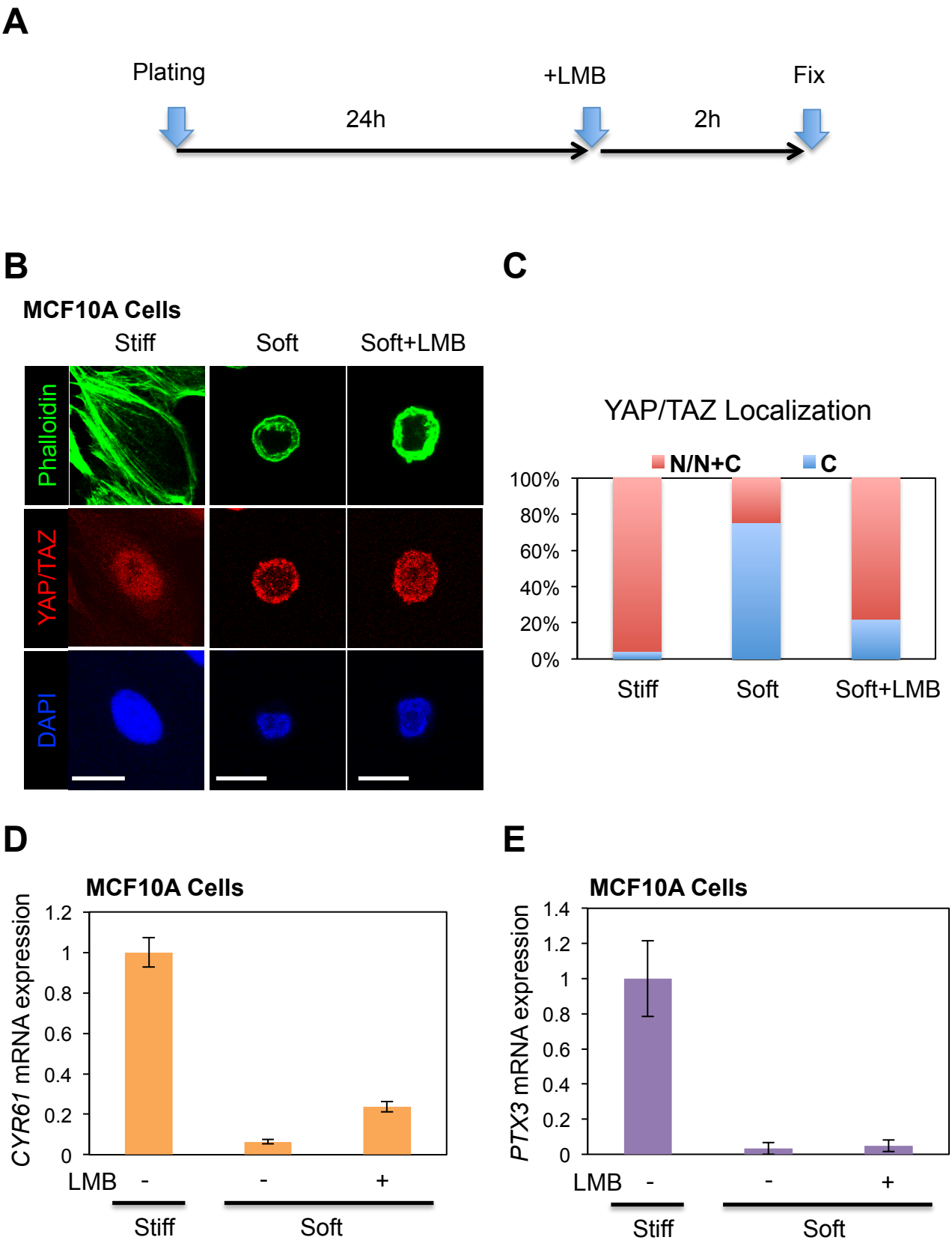
A
Plating
24h
+LMB
2h
Fix
B
MCF10A Cells
Stiff
Soft
Soft+LMB
Phalloidin
YAP/TAZ
DAPI
C
YAP/TAZ Localization
N/N+C
C
100%
80%
60%
40%
20%
0%
Stiff
Soft
Soft+LMB
D
MCF10A Cells
CYR61 mRNA expression
1.2
1
0.8
0.6
0.4
0.2
0
LMB
-
-
+
Stiff
Soft
E
MCF10A Cells
PTX3 mRNA expression
1.4
1.2
1
0.8
0.6
0.4
0.2
0
LMB
-
-
+
Stiff
Soft

Figure 5. Biochemical screening the YAP/TAZ interactors

A. Scheme of the working hypothesis on the mediator of effect of F-actin and YAP/TAZ. Two hypotheses may explain the regulation of YAP/TAZ by mechanical cues: i) the existence of a protein X activated by intact F-actin and required to sustain YAP/TAZ function; the interaction between YAP and protein X is expected to decrease upon F-actin disassembly (i.e. Lat.A treatment); or ii) the existence of protein Y inhibited by F-actin and usually functioning as a natural inhibitor of YAP/TAZ; the interaction between YAP and protein Y therefore is expected to be stabilized by disruption of the F-actin cytoskeleton.

B. Silver stain gel of proteins after **immunoprecipitation** with anti- Flag antibody in MCF10A cells stably-expressing Flag-tagged YAP 5SA or and MCF10A cells transduced with empty vector as a (negative) control, treated with Lat.A as indicated. The gel was sent to the EMBL core proteomic facility for mass spectroscopy analysis.

C. Validation of our immunoprecipitation experimental set-up described in Figure 5B. TEAD1, AMOTL2 and LATS were correctly found in the Flag-immunoprecipitation MCF10A cells stably-expressing Flag-tagged YAP 5SA .

Figure 5

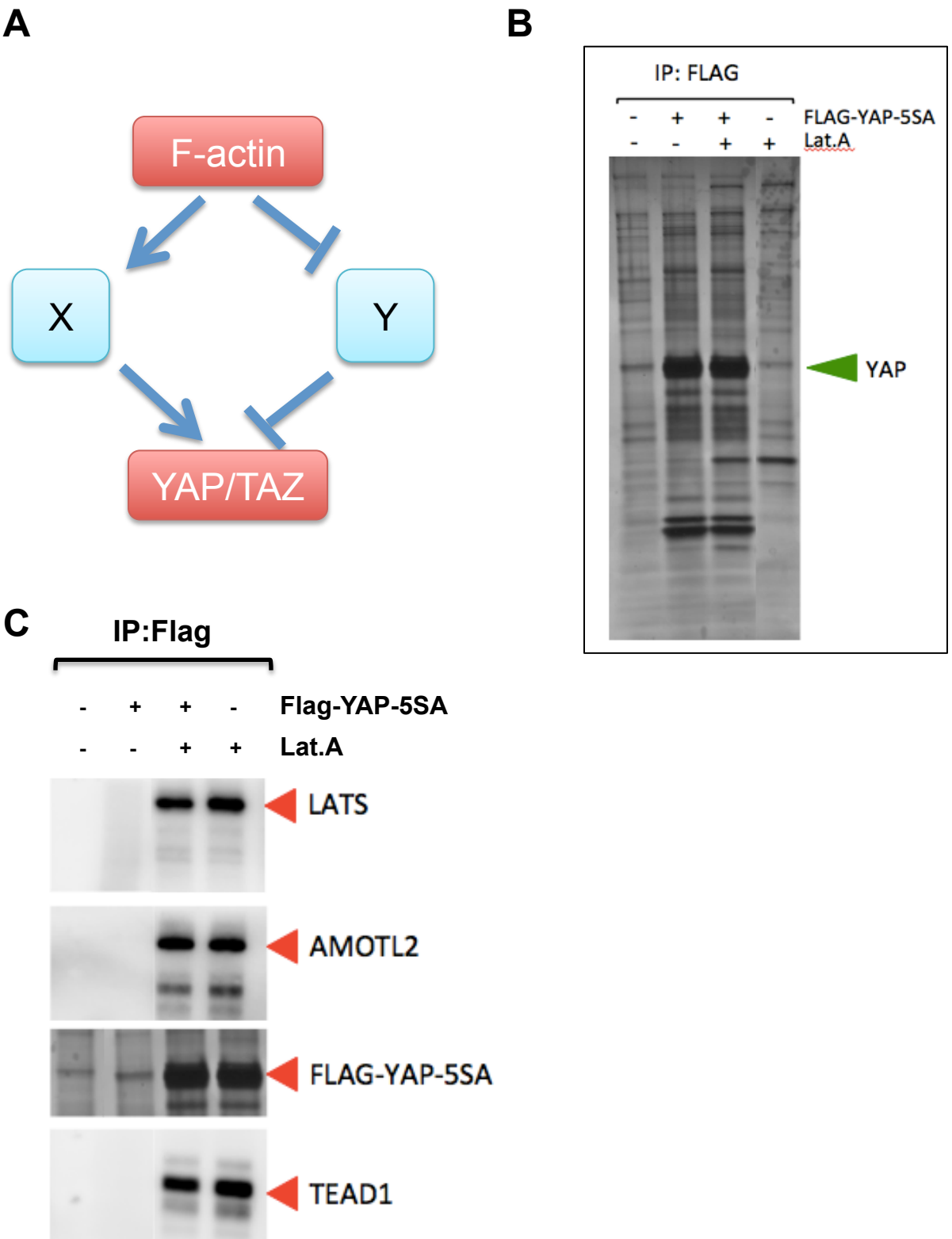
A
F-actin
X
Y
YAP/TAZ
B
IP: FLAG
- + + -
- - + +
FLAG-YAP-5SA
Lat.A
YAP
C
IP:Flag
- + + -
- - + +
Flag-YAP-5SA
Lat.A
LATS
AMOTL2
FLAG-YAP-5SA
TEAD1

Figure 6. Screening of MS results: SWI/SNF complexes work as YAP/TAZ inhibitors

A. qRT-PCR for YAP/TAZ target gene *CTGF*, normalized to *GAPDH* expression, in MCF10A cells transfected with control, ARID1A or SNF5 siRNAs as indicated. Data are normalized to control siRNA-treated cells and presented as mean + SD.

B. and C. ARID1A- and SNF5-siRNAs (used in the **Figure 6A**) knockdown efficiencies were checked by qRT-PCR. *ARID1a* and *SNF5* expression levels are relative to *GAPDH* expression.

D. qRT-PCR for *CTGF*, normalized to *GAPDH* expression, in MCF10A cells transfected with control or BRG/BRM siRNAs as indicated. Data are normalized to control siRNA-treated cells and presented as mean + SD.

E. and F. BRG1- and BRM-siRNA (used in the **Figure 6D**) knockdown efficiencies were checked by qRT-PCR. *BRG1* and *BRM* expression level are relative to *GAPDH* expression.

Figure 6

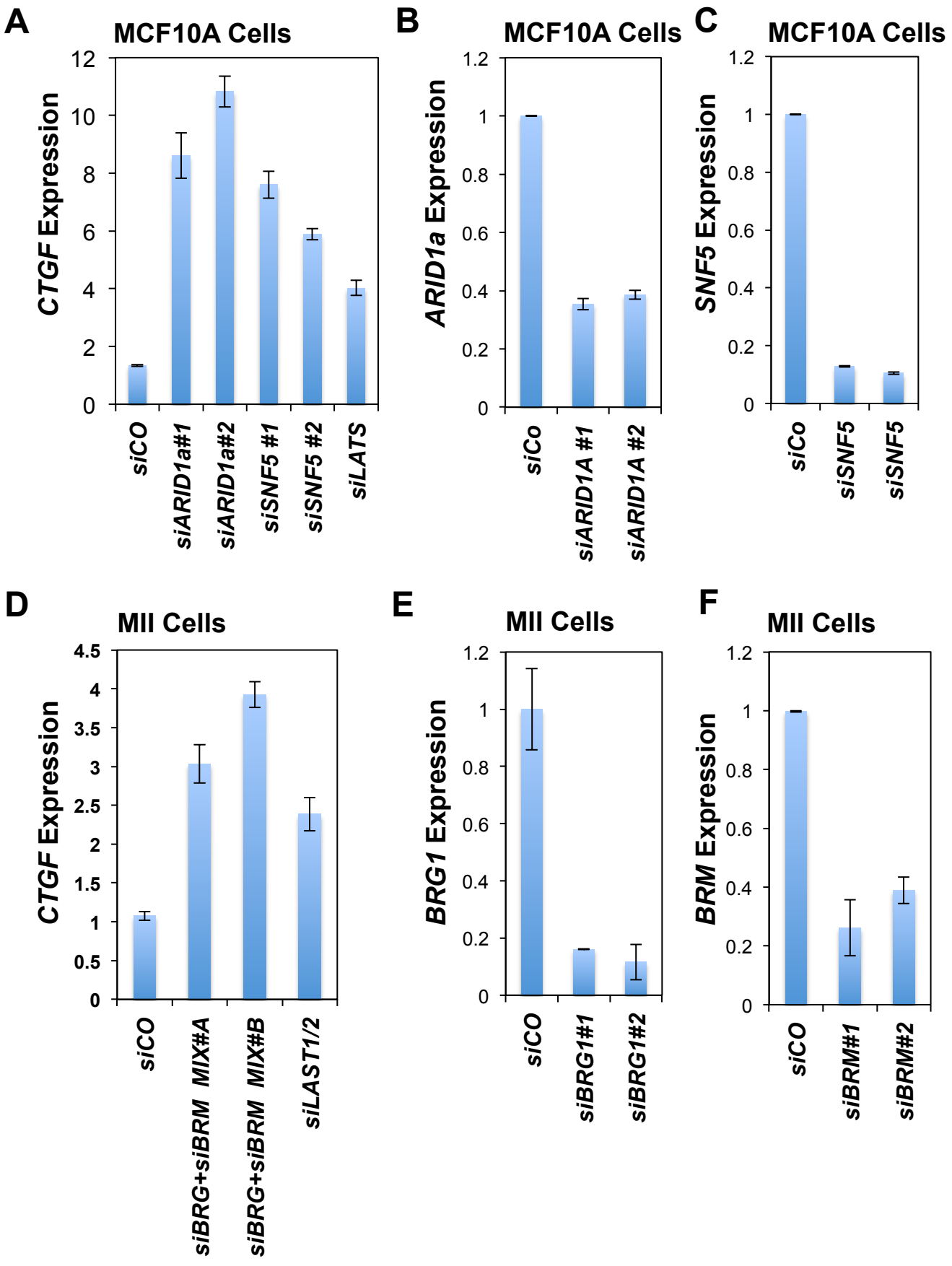
A
MCF10A Cells
CTGF Expression
12
10
8
6
4
2
0
siCO
siARID1a#1
siARID1a#2
siSNF5 #1
siSNF5 #2
siLATS
B
MCF10A Cells
ARID1a Expression
1.2
1
0.8
0.6
0.4
0.2
0
siCo
siARID1A #1
siARID1A #2
C
MCF10A Cells
SNF5 Expression
1.2
1
0.8
0.6
0.4
0.2
0
siCo
siSNF5
siSNF5
D
MII Cells
CTGF Expression
4.5
4
3.5
3
2.5
2
1.5
1
0.5
0
siCO
siBRG+siBRM MIX#A
siBRG+siBRM MIX#B
siLAST1/2
E
MII Cells
BRG1 Expression
1.2
1
0.8
0.6
0.4
0.2
0
siCO
siBRG1#1
siBRG1#2
F
MII Cells
BRM Expression
1.2
1
0.8
0.6
0.4
0.2
0
siCO
siBRM#1
siBRM#2

Figure 7. Loss of SWI/SNF complex components activate a synthetic TEAD reporter in a YAP/TAZ-dependent manner.

A. and B. HEK293 cells were left untreated (UNT) or transfected with indicated siRNAs to deplete the endogenous genes. The panels represent the results of luciferase assays with the 8xGTIIC-Lux reporter, recording YAP/TAZ-dependent transcriptional activity. Data are normalized to UNT and are presented as mean + SD.

Figure 7

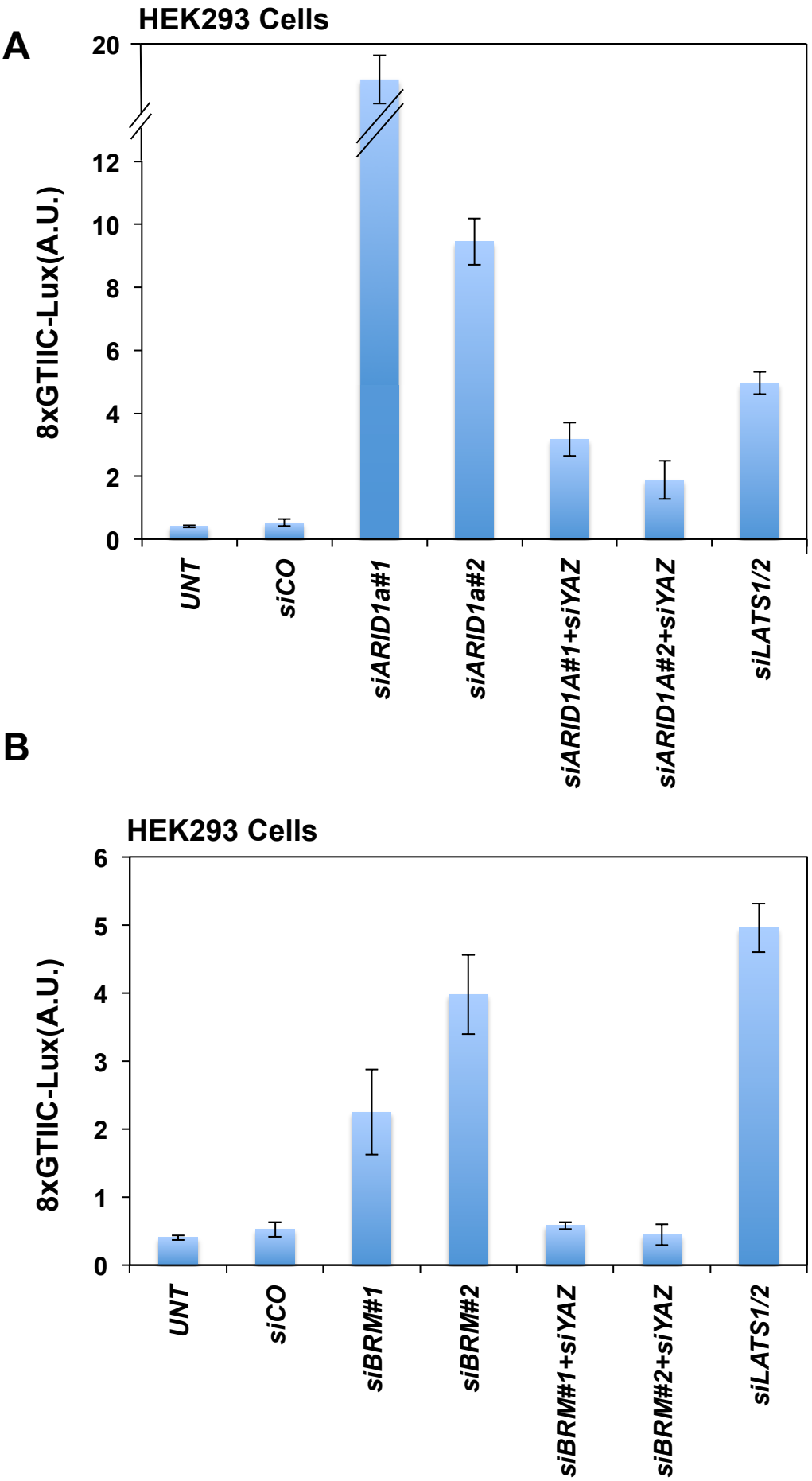
A
HEK293 Cells
8xGTIIC-Lux(A.U.)
20
12
10
8
6
4
2
0
UNT
siCO
siARID1a#1
siARID1a#2
siARID1A#1+siYAZ
siARID1A#2+siYAZ
siLATS1/2
B
HEK293 Cells
8xGTIIC-Lux(A.U.)
6
5
4
3
2
1
0
UNT
siCO
siBRM#1
siBRM#2
siBRM#1+siYAZ
siBRM#2+siYAZ
siLATS1/2

Figure 8. YAP interacts with SWI/SNF complex.

A. HEK293T cells were transfected with Flag-tagged BRM and HA-YAP 5SA. Lysates of these cells were subjected to anti-Flag immunoprecipitation and co-precipitating proteins were visualized by western blot (upper panel). The inputs were also checked by western blot (Lower panel).

B. HEK293T cells were transfected with HA-YAP 5SA and Flag-BRG1, either wild type or deleted of the HSA domain (ΔHSA). Lysates of these cells were subjected to anti-Flag immunoprecipitation and co-precipitating proteins were visualized by western blot (upper panel). The inputs were also checked by western blot (Lower panel).

C. MCF10A cells were stably transduced with Flag-YAP 5SA or with the corresponding empty vector (negative control). Lysates of these cells were subjected to anti-Flag immunoprecipitation and co-precipitating proteins were visualized by western blot.

D. Lysates from MII cells were subjected to immunoprecipitation using an anti-ARID1A antibody or rabbit IgG as control. Co-precipitating endogenous proteins were visualized by Western blot.

Figure 8

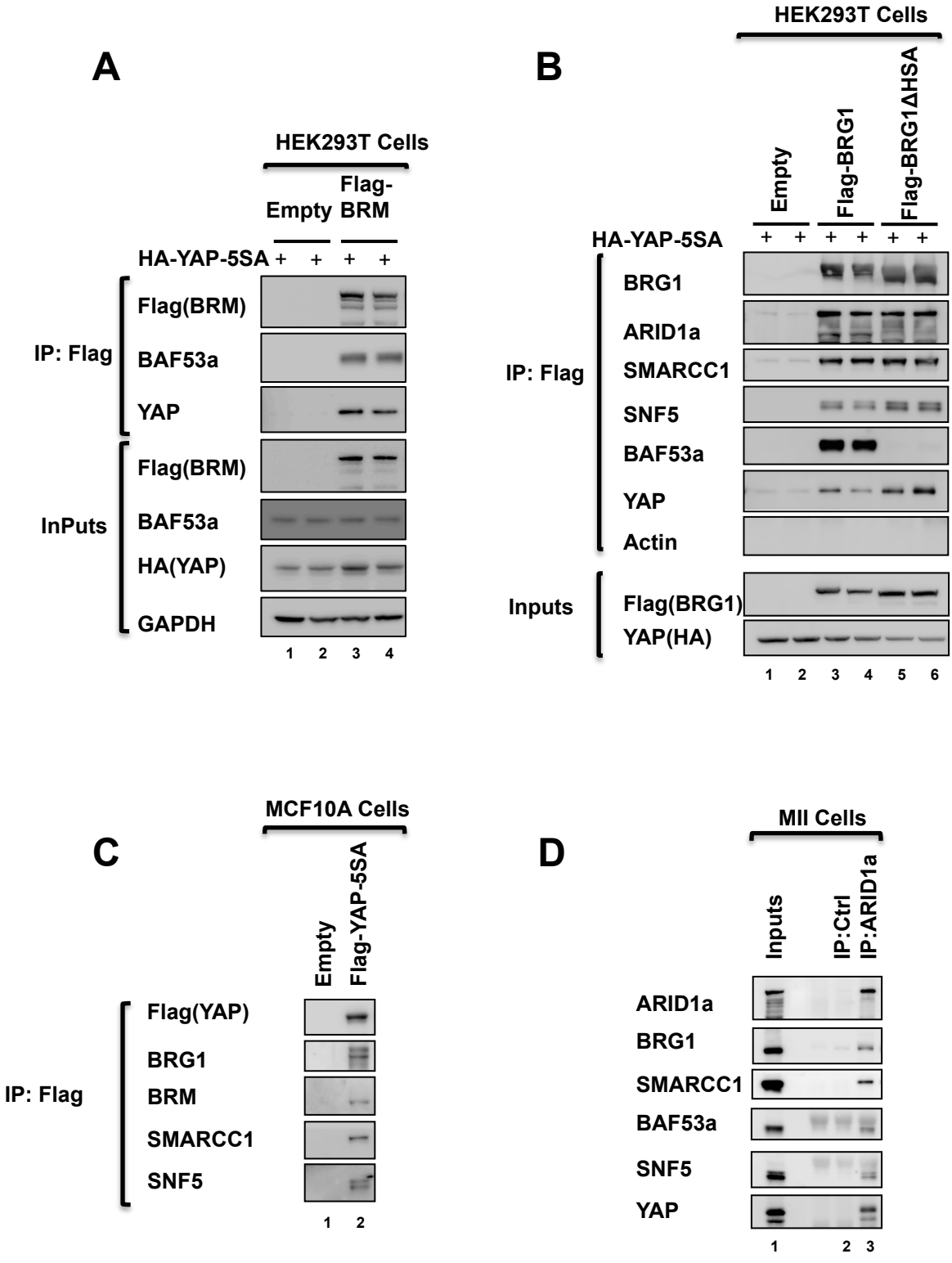
A
HEK293T Cells
Empty
Flag-BRM
HA-YAP-5SA + + + +
IP: Flag
Flag(BRM)
BAF53a
YAP
InPuts
Flag(BRM)
BAF53a
HA(YAP)
GAPDH
1 2 3 4
B
HEK293T Cells
Empty
Flag-BRG1
Flag-BRG1ΔHSA
HA-YAP-5SA + + + + + +
IP: Flag
BRG1
ARID1a
SMARCC1
SNF5
BAF53a
YAP
Actin
Inputs
Flag(BRG1)
YAP(HA)
1 2 3 4 5 6
C
MCF10A Cells
Empty
Flag-YAP-5SA
IP: Flag
Flag(YAP)
BRG1
BRM
SMARCC1
SNF5
1 2
D
MII Cells
Inputs
IP:Ctrl
IP:ARID1a
ARID1a
BRG1
SMARCC1
BAF53a
SNF5
YAP
1 2 3

Figure 9. YAP directly binds to ARID1a.

A. HEK293T cells were transfected with two independent control siRNAs (lanes 1, 2 and lanes 3, 4) or with mixed siRNAs against BRG1 and BRM (lanes 5, 6). Lysates of these cells were subjected to IP using an anti-ARID1a antibody or rabbit IgG as control, and co-precipitating endogenous proteins were detected by western blot. The lower panel shows the inputs of co-IP experiment.

B. HEK293T cells were transfected with independent siRNA for indicated genes (ARID1a in lanes 5 and 6; BAF53a in lanes 7 and 8; SNF5 in lanes 9 and 10) and siRNA control (in lanes 1, 2, 3 and 4) and with plasmid encoding Flag-BRG1 as indicated. Cell lysates were subjected to anti-Flag immunoprecipitation and co-precipitating endogenous proteins were checked by western blot. The inputs were checked by western blot (the lower panel).

Figure 9

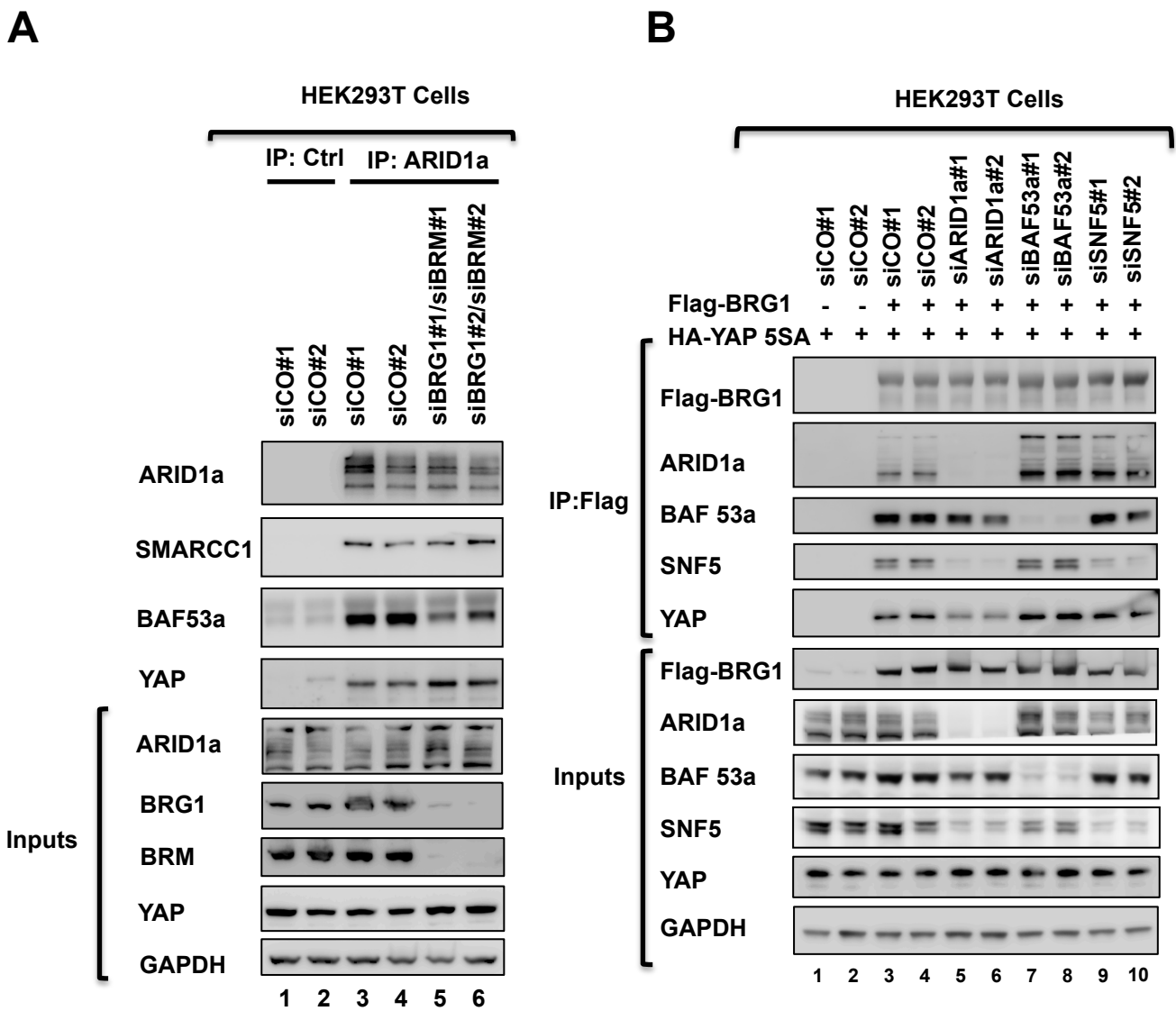
A
HEK293T Cells
IP: Ctrl
IP: ARID1a
siCO#1
siCO#2
siCO#1
siCO#2
siBRG1#1/siBRM#1
siBRG1#2/siBRM#2
ARID1a
SMARCC1
BAF53a
YAP
Inputs
ARID1a
BRG1
BRM
YAP
GAPDH
1 2 3 4 5 6
B
HEK293T Cells
siCO#1
siCO#2
siCO#1
siCO#2
siARID1a#1
siARID1a#2
siBAF53a#1
siBAF53a#2
siSNF5#1
siSNF5#2
Flag-BRG1 - - + + + + + + + +
HA-YAP 5SA + + + + + + + + + +
IP:Flag
Flag-BRG1
ARID1a
BAF 53a
SNF5
YAP
Inputs
Flag-BRG1
ARID1a
BAF 53a
SNF5
YAP
GAPDH
1 2 3 4 5 6 7 8 9 10

Figure 10. YAP binds to ARID1a through its WW domain.

A. Schematic representation depicting the multiple domains of YAP, and mapping the interactions with other proteins (Piccolo et al., 2014). The domains of YAP are presenting from C-terminal to N-terminal: PDZ Binding motif, TAD (Transcription Activation Domain), Coiled-Coil Domain, WW domain, TEAD Interacting Domain.

B. Schematic representation of YAP deletion and mutation constructs used for the experiment depicted in Figures 10 C, D.

C. HEK293T cells were transfected with the indicated YAP deletion constructs (Flag-tagged) described in Figure 10B. Protein extracts were subjected to anti-Flag IP and analyzed for coprecipitating endogenous ARID1A, BRG1, SNF5, AMOT, PTPN14 and TEAD4.

D. HEK293T cells were transfected with the indicated YAP deletion or mutation constructs (Flag-tagged) described in Figure 10B. Protein extracts were subjected to anti-Flag IP and analyzed for coprecipitating endogenous ARID1a, SNF5, AMOT, PTPN14 and TEAD4.

Figure 10

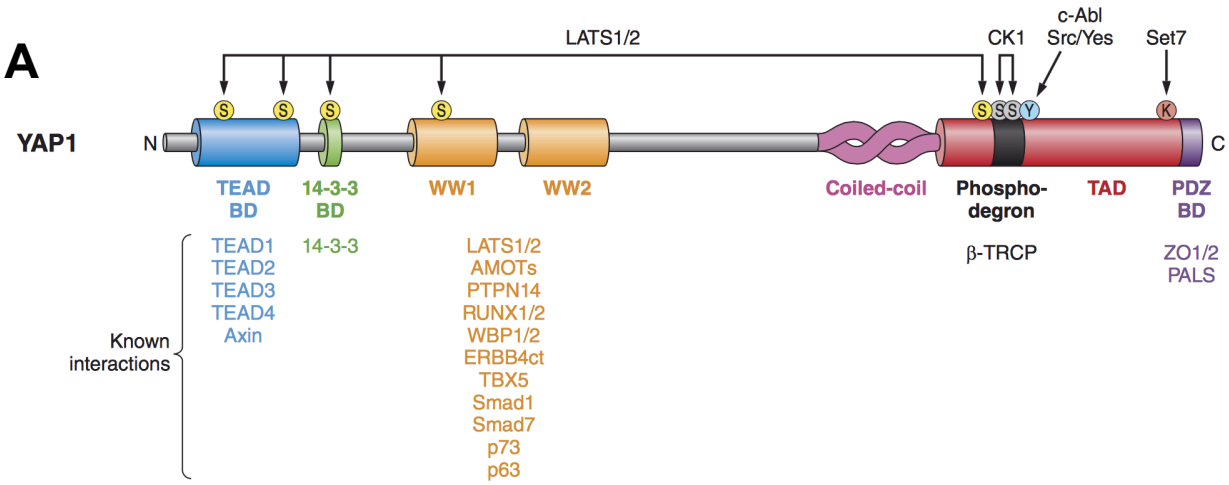
A
YAP1
N
C
LATS1/2
CK1
c-Abl
Src/Yes
Set7
TEAD BD
14-3-3 BD
WW1
WW2
Coiled-coil
Phospho-degron
TAD
PDZ BD
β-TRCP
ZO1/2
PALS
Known interactions
TEAD1
TEAD2
TEAD3
TEAD4
Axin
14-3-3
LATS1/2
AMOTs
PTPN14
RUNX1/2
WBP1/2
ERBB4ct
TBX5
Smad1
Smad7
p73
p63

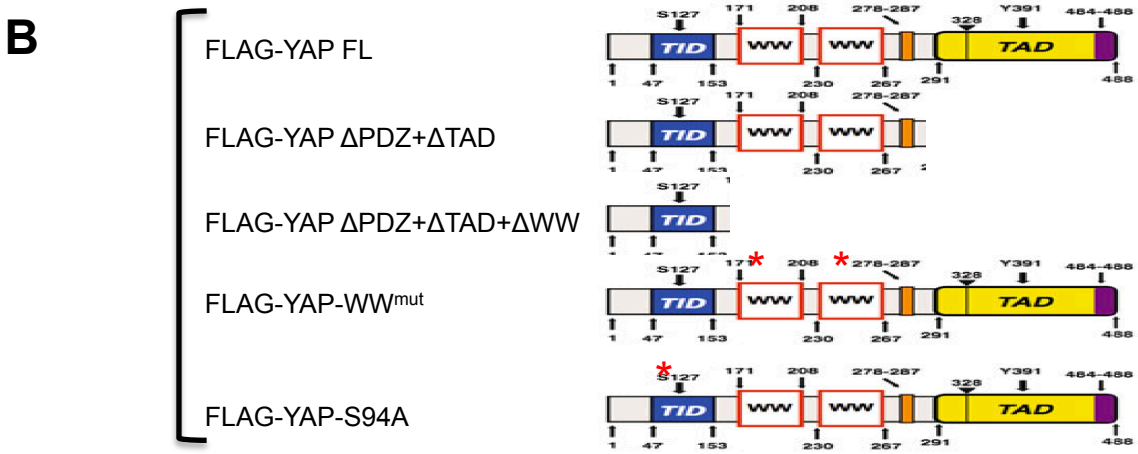
B
FLAG-YAP FL
FLAG-YAP ΔPDZ+ΔTAD
FLAG-YAP ΔPDZ+ΔTAD+ΔWW
FLAG-YAP-WWmut
FLAG-YAP-S94A
TID
WW
TAD

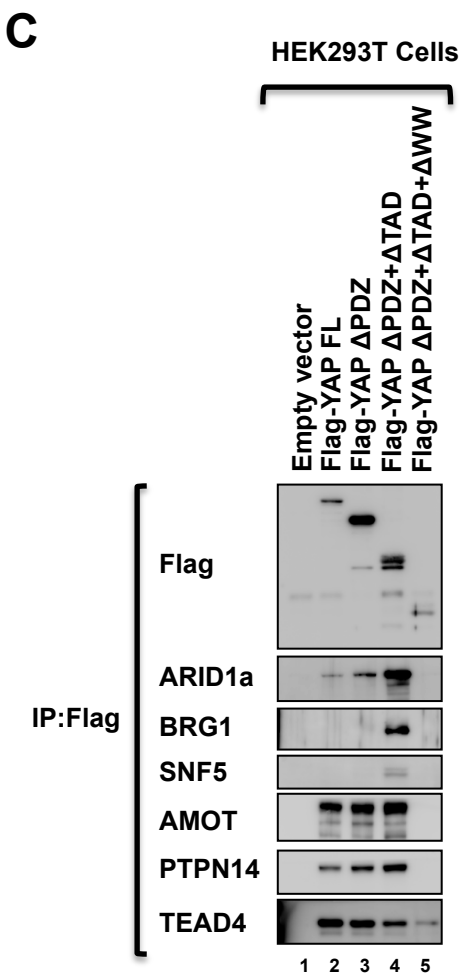
C
HEK293T Cells
Empty vector
Flag-YAP FL
Flag-YAP ΔPDZ
Flag-YAP ΔPDZ+ΔTAD
Flag-YAP ΔPDZ+ΔTAD+ΔWW
IP:Flag
Flag
ARID1a
BRG1
SNF5
AMOT
PTPN14
TEAD4
1 2 3 4 5

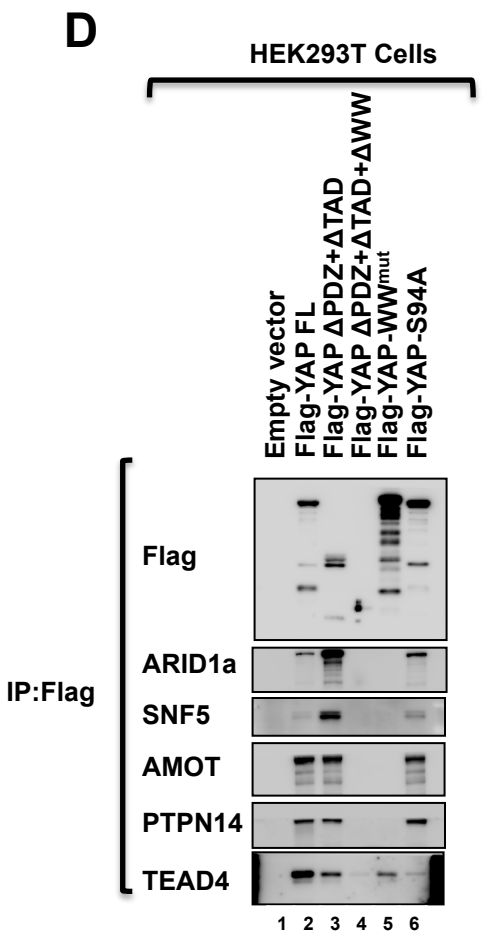
D
HEK293T Cells
Empty vector
Flag-YAP FL
Flag-YAP ΔPDZ+ΔTAD
Flag-YAP ΔPDZ+ΔTAD+ΔWW
Flag-YAP-WWmut
Flag-YAP-S94A
IP:Flag
Flag
ARID1a
SNF5
AMOT
PTPN14
TEAD4
1 2 3 4 5 6

Figure 11. F-actin binding to SWI/SNF causes YAP to dissociate from SWI/SNF

A. Schematic representation of experiment depicted in **Figure 11B**.

B. HEK293T cells were either left untreated or treated with Lat.A. Bio-Phall was added to the lysates after harvesting. Lysates were then subjected to Bio-Phall pulldown using streptavidin resin. Precipitating proteins were visualized by western blot. Inputs are shown in lane 1.

C. MII cells were treated with either Lat.A or Phalloidin (Phall) for 4 hours. Lat.A or Phall were kept present in the lysates throughout all the following passages. Lysates were subjected to IP by using an anti-YAP antibody or rabbit IgG as control. Co-precipitating endogenous proteins were detected by western blot. Inputs were checked by western blot (lanes 5 and 6).

D. MII cells were transfected with independent control siRNAs (lanes 1, 2 and 3, 4) or siRNAs against ARID1A (lanes 5 and 6) and treated with Lat.A or Phall as indicated. Lysates were then subjected to IP by using an anti-YAP antibody or rabbit IgG as control. Co-precipitating endogenous proteins were detected by western blot. Inputs were checked by western blot (lower panel).

Figure 11

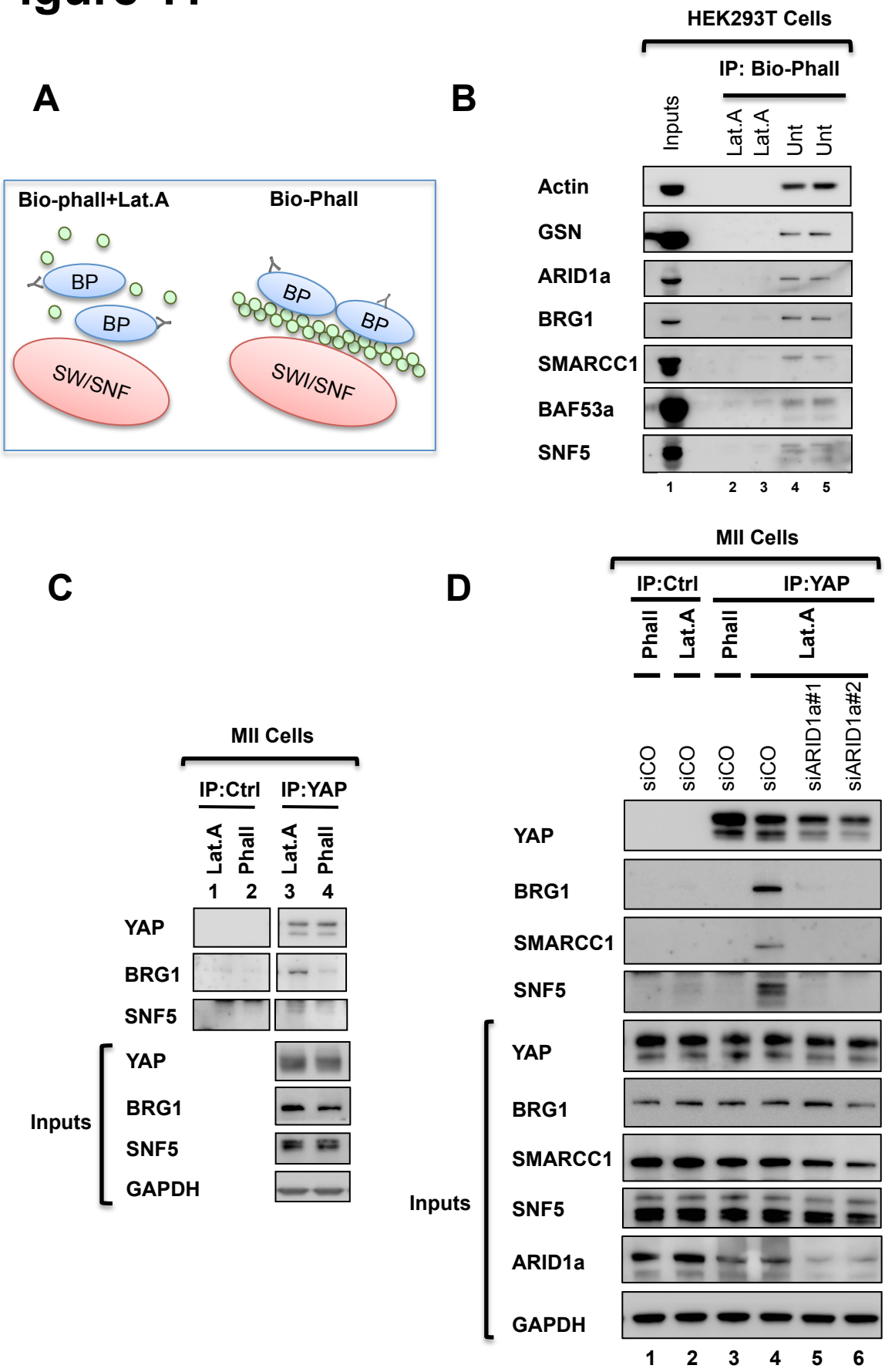
A
Bio-phall+Lat.A
Bio-Phall
BP
BP
SW/SNF
BP
BP
SWI/SNF
B
HEK293T Cells
IP: Bio-Phall
Inputs
Lat.A
Lat.A
Unt
Unt
Actin
GSN
ARID1a
BRG1
SMARCC1
BAF53a
SNF5
1 2 3 4 5
C
MII Cells
IP:Ctrl
IP:YAP
Lat.A
Phall
Lat.A
Phall
1 2 3 4
YAP
BRG1
SNF5
Inputs
YAP
BRG1
SNF5
GAPDH
D
MII Cells
IP:Ctrl
IP:YAP
Phall
Lat.A
Phall
Lat.A
siCO
siCO
siCO
siCO
siARID1a#1
siARID1a#2
YAP
BRG1
SMARCC1
SNF5
Inputs
YAP
BRG1
SMARCC1
SNF5
ARID1a
GAPDH
1 2 3 4 5 6

Figure 12. Knockdown of ARID1a rescues YAP activity in mechanically-inhibited cells

A. Schematic representation of the experiment of Figures 12 B, C.

B. and C. Loss of *ARID1a* rescues YAP/TAZ transcriptional activity in dense monolayers. MCF10a cells were transfected with independent siRNAs against ARID1a and with control siRNA. Then cells were seeded to obtain sparse cells or a dense monolayer. LMB were added to the cells two hours before harvesting for RNA. *CTGF* and *CYR61* mRNA levels were checked by qRT-PCR and are normalized to GAPDH expression.

D. and E. Loss of *ARID1a* rescues YAP/TAZ transcriptional activity in soft ECM. MCF10A cells were transfected with independent siRNAs against ARID1a and with control siRNA. Next, cells were seeded on a stiff substrate or a soft substrate. Then cells were harvest for RNA extraction. *CTGF* and *PTX3* mRNA levels were checked by qRT-PCR and are normalized to GAPDH expression.

Figure 12

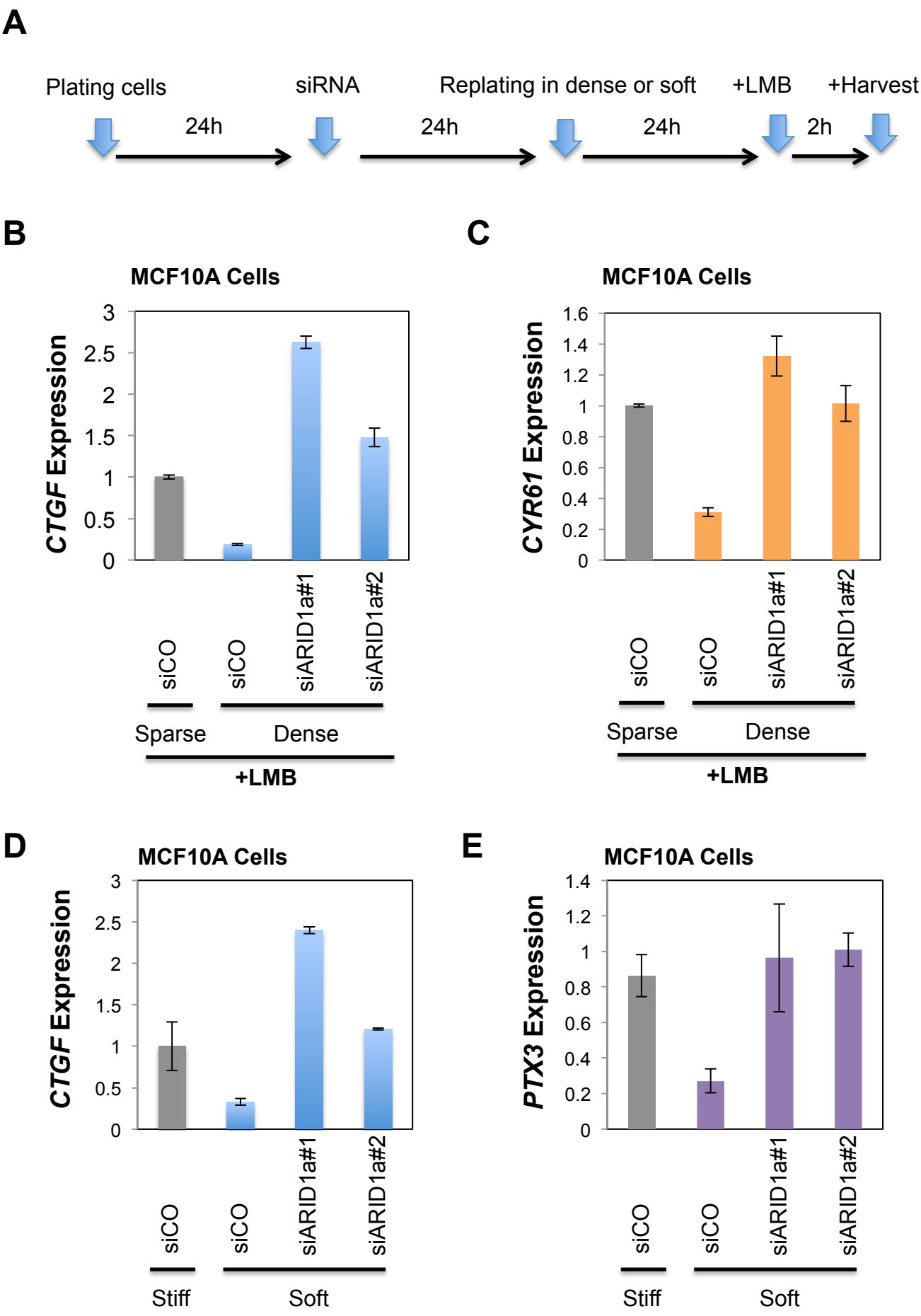
A
Plating cells
24h
siRNA
24h
Replating in dense or soft
24h
+LMB
2h
+Harvest
B
MCF10A Cells
CTGF Expression
siCO
siCO
siARID1a#1
siARID1a#2
Sparse
Dense
+LMB
C
MCF10A Cells
CYR61 Expression
siCO
siCO
siARID1a#1
siARID1a#2
Sparse
Dense
+LMB
D
MCF10A Cells
CTGF Expression
siCO
siCO
siARID1a#1
siARID1a#2
Stiff
Soft
E
MCF10A Cells
PTX3 Expression
siCO
siCO
siARID1a#1
siARID1a#2
Stiff
Soft

Figure 13. SWI/SNF complexes work as YAP inhibitors in Neurons

A. Schematic representation of the experiment of Figure 13B. Neurons plated on plastic were infected with lentiviruses encoding for tetO-YAP and rtTA. Mature neurons were selected by culturing them in neuronal medium containing the anti-mitotic drug AraC. After selection, neurons were infected with lentiviruses encoding the indicated shRNA (shCo, *shBrm* or *shArid1a*). After 24 hours of infection, medium was changed to NSC medium supplemented with doxycycline (see Methods). Generally, 15 days after inducing exogenous YAP in neurons, reprogrammed "NSC-like" spheres could be counted.

B. Representative images of neurospheres formed in the different conditions.

C. Quantification of the number of neurospheres formed by each of the samples depicted in Figure 13**B**.

D. *shArid1a* and *shBrm* knockdown efficiencies in neurons were checked by qRT-PCR.

Figure 13

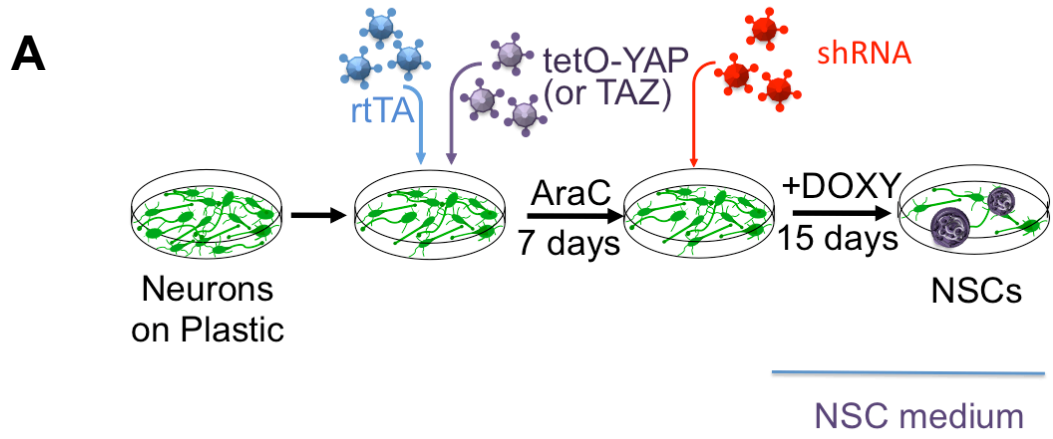
A
rtTA
tetO-YAP
(or TAZ)
shRNA
AraC
7 days
+DOXY
15 days
Neurons
on Plastic
NSCs
NSC medium

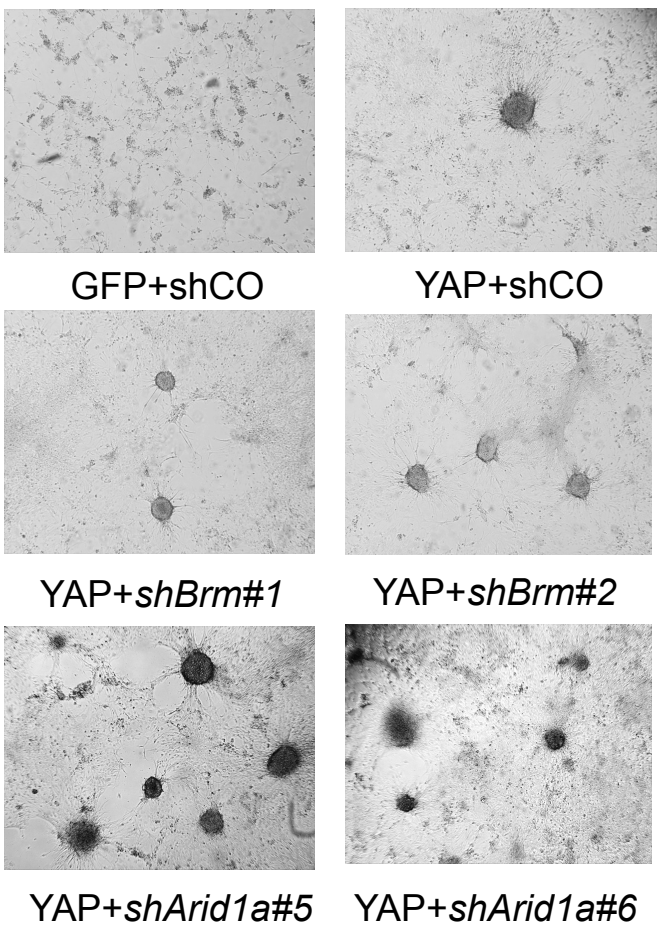
B
GFP+shCO
YAP+shCO
YAP+shBrm#1
YAP+shBrm#2
YAP+shArid1a#5
YAP+shArid1a#6

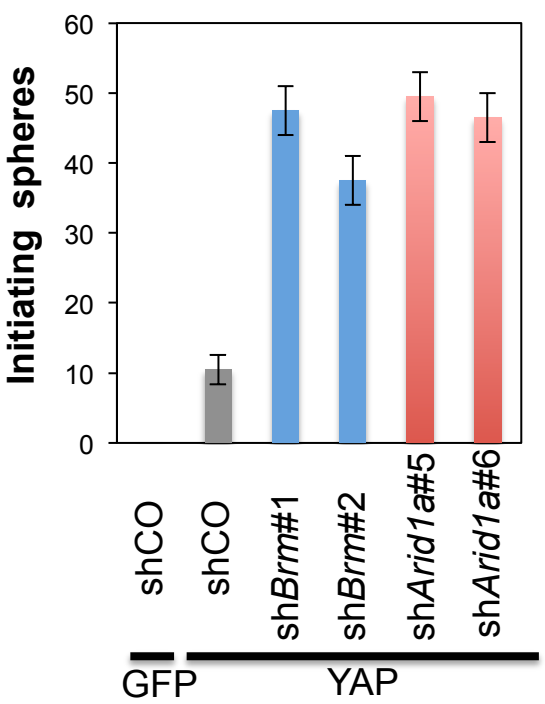
C
Initiating spheres
60
50
40
30
20
10
0
shCO
shCO
shBrm#1
shBrm#2
shArid1a#5
shArid1a#6
GFP
YAP

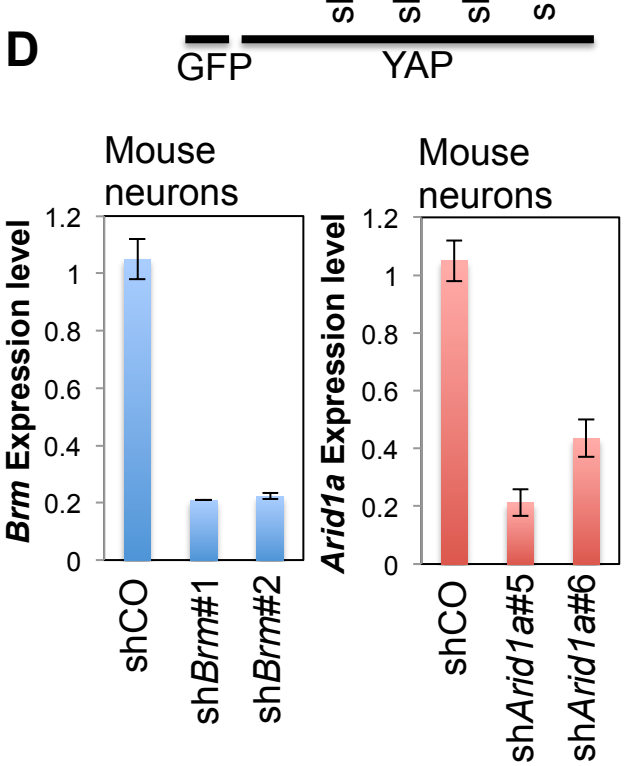
D
Mouse neurons
Brm Expression level
1.2
1
0.8
0.6
0.4
0.2
0
shCO
shBrm#1
shBrm#2
Mouse neurons
Arid1a Expression level
1.2
1
0.8
0.6
0.4
0.2
0
shCO
shArid1a#5
shArid1a#6

Figure 14. YAP-induced reprogramming is under mechanical regulation

A. Schematic overview of YAP-induced reprogramming in neurons plated either on stiff substrate or on soft substrate.

B, C. Representative images (B) and quantifications (C) of "NSC-like" neurospheres formed by YAP-expressing neuron plated on stiff substrate or on soft substrate.

Figure 14

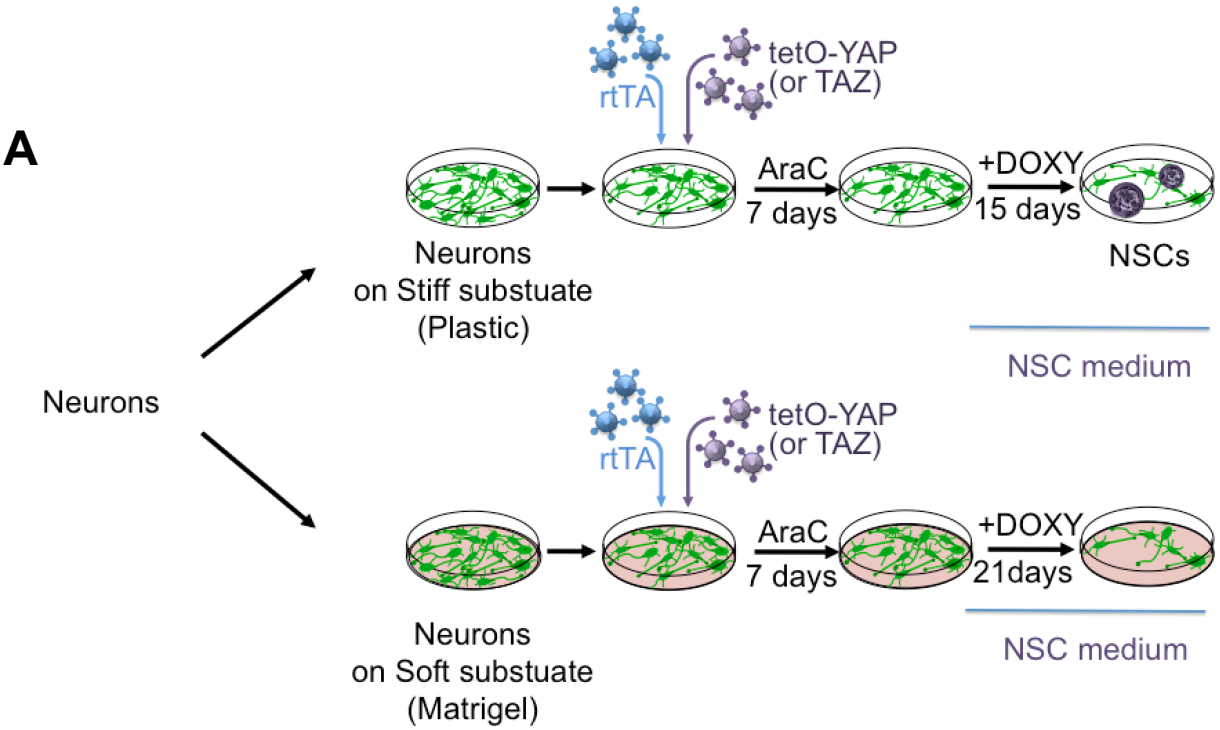

B

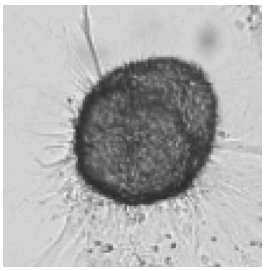

Stiff

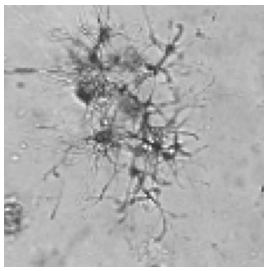

Soft

C

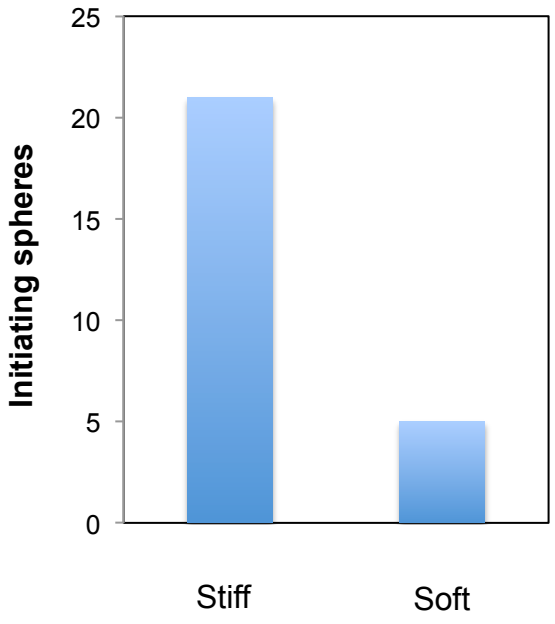

Figure 15. Loss of SWI/SNF complex could help YAP to overcome mechanoregulation.

A. Schematic overview of YAP-induced reprogramming of neurons plated on a soft substrate.

B. Representative images and quantifications of neurospheres formed by Arid1a-depleted neurons after YAP-induced reprogramming.

C. Representative images and quantifications of neurospheres formed by Brm-depleted neurons after YAP-induced reprogramming.

Figure 15

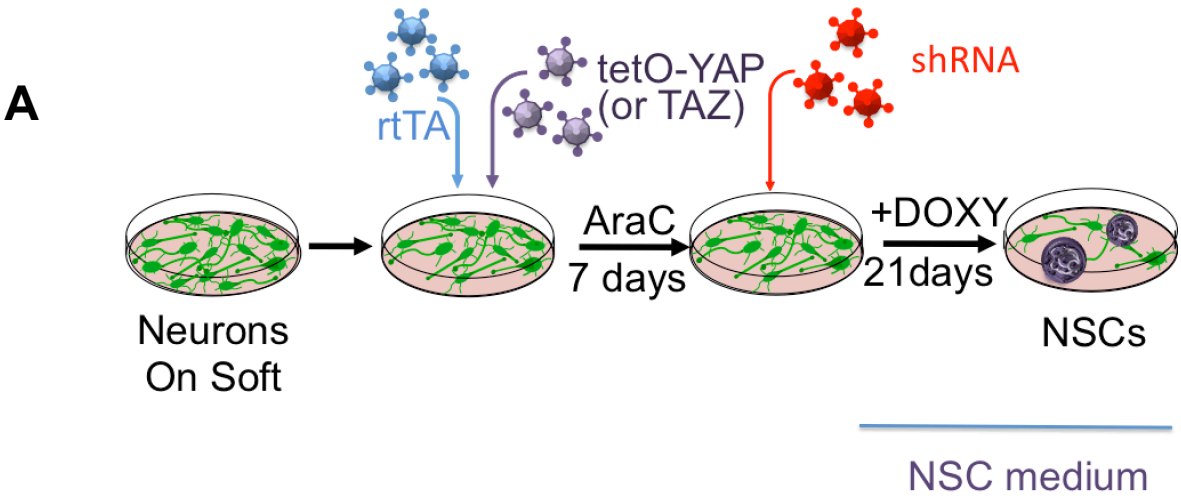
A
rtTA
tetO-YAP
(or TAZ)
shRNA
AraC
7 days
+DOXY
21days
Neurons
On Soft
NSCs
NSC medium

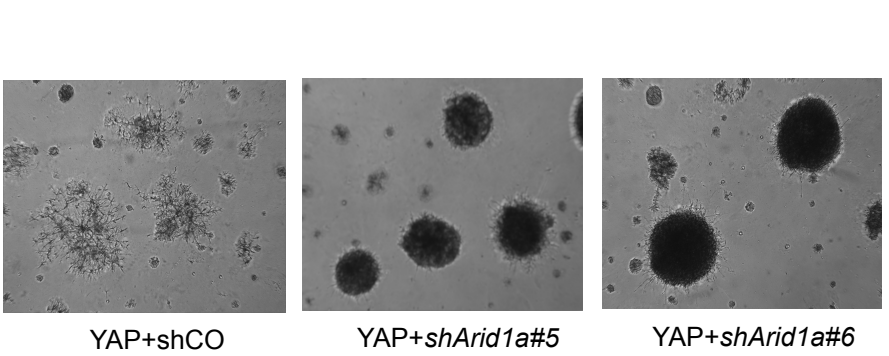
B
YAP+shCO
YAP+shArid1a#5
YAP+shArid1a#6

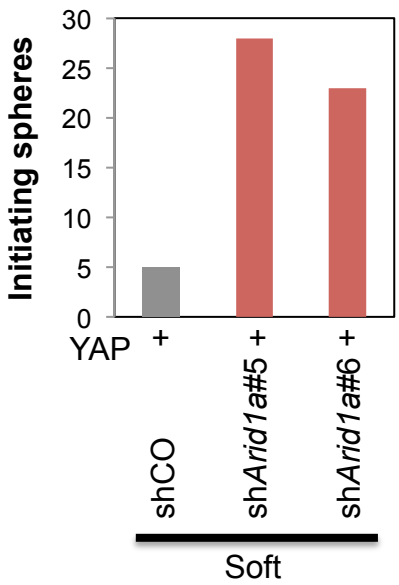
Initiating spheres
30
25
20
15
10
5
0
YAP + + +
shCO
shArid1a#5
shArid1a#6
Soft

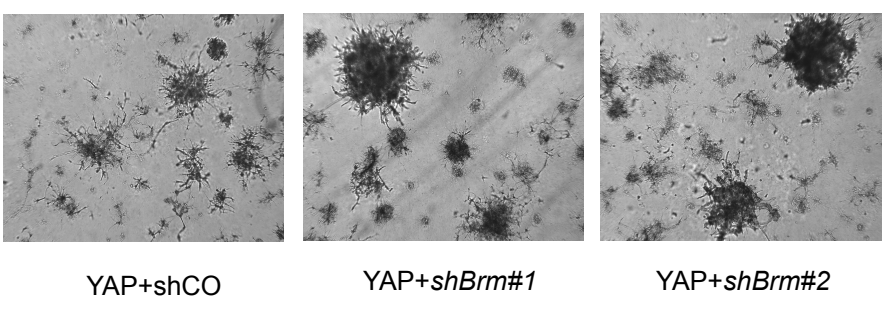
C
YAP+shCO
YAP+shBrm#1
YAP+shBrm#2

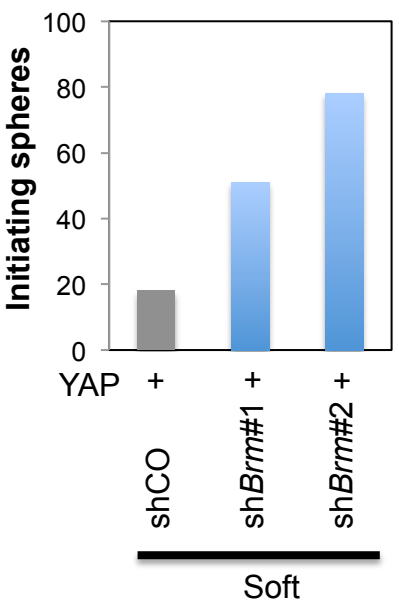
Initiating spheres
100
80
60
40
20
0
YAP + + +
shCO
shBrm#1
shBrm#2
Soft

Figure 16. Loss of SWI/SNF complex facilitate YAP induced reprogramming and overcome mechanoregulation.

Immunofluorescence for the neuron marker NeuN and neuron stem cell marker SOX2 during YAP-induced reprogramming in the indicated conditions.

Figure 16

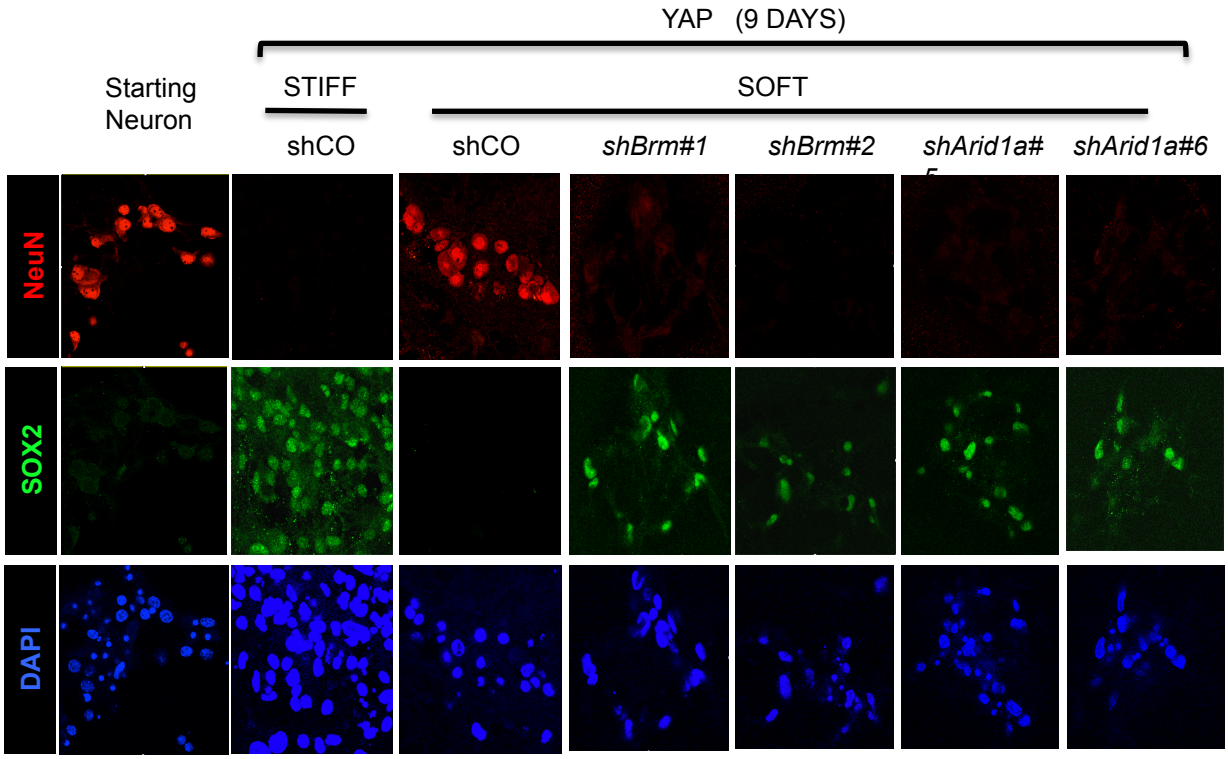
YAP (9 DAYS)
Starting Neuron
STIFF
SOFT
shCO
shCO
shBrm#1
shBrm#2
shArid1a#
shArid1a#6
NeuN
SOX2
DAPI